An Experimental Investigation of Unbraced Reinforced Concrete Frames

Nourollah Samiee Nejad
Portland State University

AN ABSTRACT OF THE THESIS OF Nourollah Samiee Nejad for the Master of

Science in Applied Science presented May 20, 1977.

Title: An Experimental Investigation of Unbraced Reinforced Concrete

Frames

APPROVED BY MEMBERS OF THE THESIS COMMITTEE:

Franz, N. Rad, Chairman

Wendelin H. Mueller, III

Frank P. Terraglio

Phillip J. Gold

The main objective of this investigation is to study experimentally

the behavior of rectangular reinforced concrete frames subject to a

combination of low column loads, beam loads, and lateral load. The

analytical tool used in this investigation is a computer program which

is a generalized computational method for non linear force deformation

relationship and secondary forces due to displacement of the joints

during loading.

In the experimental portion of this investigation, two rectangular

frames, one design by the Ultimate Strength Design method and the other

by a Limit Design method were prepared and tested to failure with short time loading.

Physical tests indicate that frames under the action of low gravity loads and lateral load became unstable after the formation of two hinges in the beams.

AN EXPERIMENTAL INVESTIGATION OF

UNBRACED REINFORCED CONCRETE FRAMES
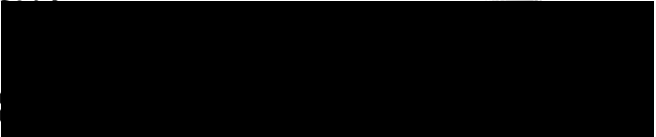
by

Nourollah Samiee Nejad

A thesis submitted in partial fulfillment of the
requirements for the degree of

MASTER OF SCIENCE
in
APPLIED SCIENCE

Portland State University
1977

TO THE OFFICE OF GRADUATE STUDIES AND RESEARCH:
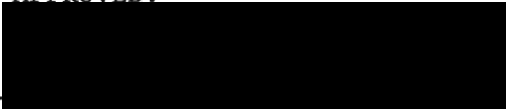
The members of the Committee approve the thesis of Nourollah Samiee Nejad presented May 2Q 1977.

Franz N. Rad, Chairman

Wendelin H. Mueller, III

Phillip J. Qold

APPROVED:

Fred M. Young, Head, Department of Engineering and Applied Science

Stanley E. Rauch, Dean of Graduate Studies and Research

TO MY PARENTS

Mohamad-Hossien Samiee Nejad
and
Khojasteh Samiee Nejad

ACKNOWLEDGMENTS

TABLE OF CONTENTS

PAGE

LIST OF TABLES

LIST OF FIGURES

CHAPTER I

INTRODUCTION

1.1 GENERAL

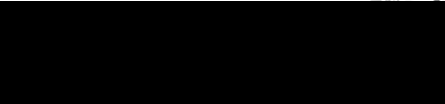Although some of the early investigators of reinforced concrete favored design based on ultimate strength theories, working stress design (elastic theory) method was long the standard design procedure. In 1956, the ACI code authorized design based on ultimate strength. As compared to working stress design, ultimate strength design theory results in a more uniform factor of safety, a greater saving of material, and a more consistant design procedure. In 1964, the European Concrete Committee introduced the concept of limit state design [1]. Mainly limit design method aims to satisfy three conditions: (1) limit equilibrium, (2) rotational compatibility, (3) serviceability.

This method of design takes the elastic moment pattern method (assumed by working stress and ultimate strength design methods) a stage further and allows moment redistribution.

1.2 REINFORCED CONCRETE BEHAVIOR BEYOND THE ELASTIC STAGE

To understand the behavior of any structure, behavior of its components such as beams and columns, and the materials used in the structure must be well understood. There has been a large number of investigations both analytically and experimentally on the behavior of reinforced concrete members and frames in recent years and a few are summarized below:

In 1961 a report on limit design was published by the Institution Research Committee on Ultimate Load Design. In this report, the fundamental theory and application of limit design were reviewed and a design method suggested. In this method, positions of plastic hinges and the values of rotation at hinges in a structure are obtained by a trial and adjustment procedure (2).

Limit design theories for reinforced concrete statically indeterminate structures require a knowledge of rotation capacity of hinging regions. Results of thirty-seven tests of double reinforced beams (3) showed that maximum concrete compressive strain was very much in excess of the usually assumed value of .003. Consequently, the curvature at ultimate strength can also be very much greater than the value calculated on the assumption that the maximum concrete compressive strain is limited to .003. So the inelastic rotation occuring in the hinging regions was considerably greater than might be expected.

In 1968, ACI-ASCE Committee 428 Limit Design, submitted a report on "Model Code Clauses" (4) based on recent developments on nonlinear behavior of reinforced concrete structures. The suggested model clauses defined envelopes, or upper and lower limits, rather than a single method of design.

There also has been extensive research on the strength of long reinforced concrete columns in recent years (5,6). Some investigations have particularly focused on framed columns. In unbraced frames, moments due to lateral deflection of frame may become very significant. In a recent investigation (7), the behavior of single story two column reinforced concrete frames under combined loading was studied. The re-

sults indicated that the frames under the action of large gravity loads and lateral load become unstable after the formation of two hinges at leeward joints, either in the ends of column or the adjacent beam.

1.3   OBJECTIVES OF THIS INVESTIGATION

The main objective of this investigation was to study experimentally the behavior of rectangular reinforced concrete frames, subjected to a combination of low column loads, beam loads, and lateral loads.

The main portion of this investigation may be outlined as follows:

1)   To describe the design and loading condition of the test frames, discussed in Chapter II.

2)   To describe the design and fabrication of the loading system, discussed in Chapter III.

3)   To describe the physical test behavior of two frames and the predicted behaviors by a computer analysis. This portion is explained in Chapter IV.

Chapter V contains a summary and conclusions of this investigation.

CHAPTER II

ANALYTICAL APPROACH

2.1 GENERAL

The main purpose of this investigation was to determine physical behavior of two unbraced rectangular reinforced concrete frames, one designed by the ultimate strength design method and the other by a limit design method.

An unbraced multistory structure is shown in Fig. 2.1. One portion of this structure (one story, one bay) as shown in Fig. 2.2 (a,b) represents the behavior of each panel. This panel is acted upon by column loads, floor loads shown as two concentrated loads (Q) at beam third points, and wind (or earthquake) load. Since this frame is anti-symmetrical with respect to a horizontal axis through the mid height of the column, only the top half of the frame is selected for analytical and experimental work in this investigation.

2.2 GENERAL NONLINEAR PROGRAM NØNFIX7

The main analytical tool used in this investigation was computer program "NØNFIX7", which is a modified version of the computer program "NØNFIX5" developed by Gunnin (8). Program NONFIX7 is a generalized computational method for a nonlinear force-deformation relationship and secondary forces due to displacement of the joints during loading. The thrust-moment-curvature relationships for individual members are constructed using a subroutine which assumes Hognestad (9) stress-strain
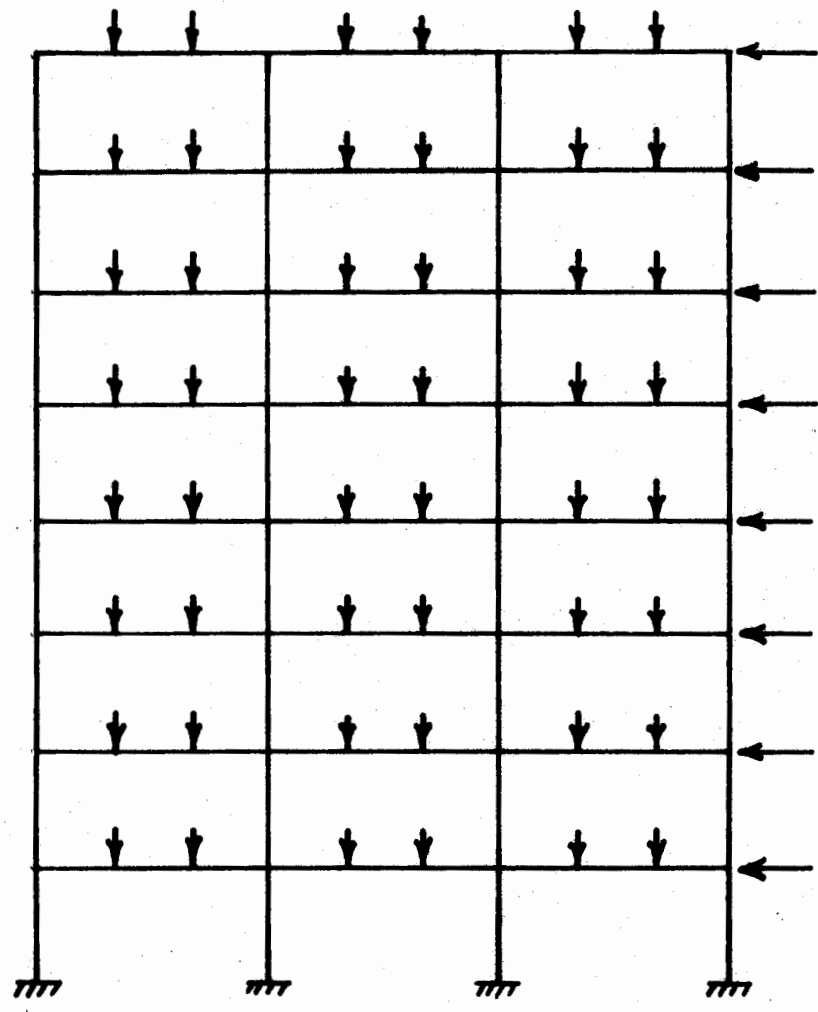
Figure 2.1 Multistory unbraced frame
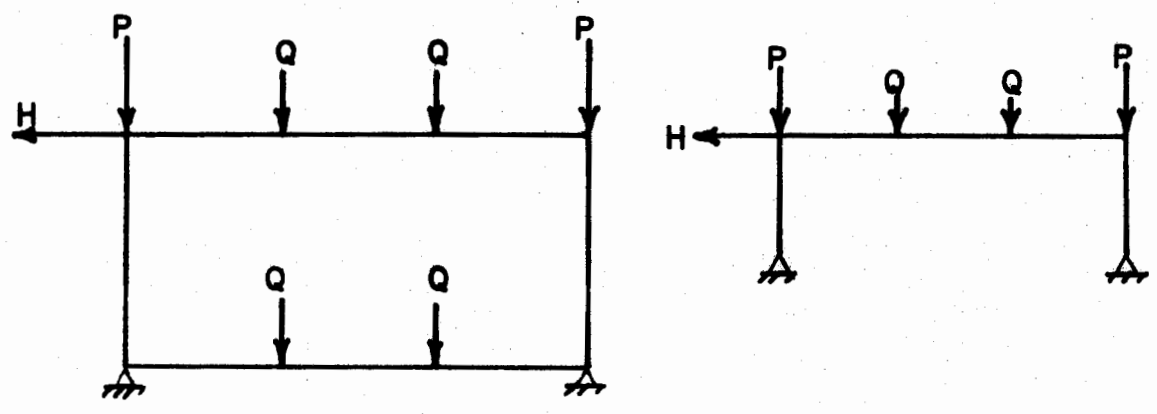
Figure 2.2 Panel and model frame

curve for steel in tension and compression. A complete description of this computer program can be found in Ref. (7) and Ref. (8).

2.3   FRAME SELECTION

a)   General - Several test frames were analyzed using a non-linear computer program and a model study. A recent model study (7) indicated that as the number of stories increase, thus increasing column thrusts, a condition of frame stability failure may result. Computer analyses (11) indicated that the number of stories should not go above 6 or 7, if limit design is to be used for design of unbraced concrete frames. Accordingly, test frames representing the lowest level of a seven story structure were selected. Figure 2.1 shows a seven story structure with floor loads and lateral loads. The relationships $Q/T = 1/(2n-1)$, and $Q/P = 1/(2n-2)$ exist between gravity loads, where   Q is the beam load at third point, T is column thrust, P is column load (applied at top), n is number of stories. Based on the above relationship, for n = 7, a Q/P of 0.083 was selected for the test frames.   Frames USD-2 and LD-2 were designed by Gavin (11).

b) Frame USD-2 - The assumed service loads are shown in Fig. 2.3. The ACI 318-71 (10) code equations 9-1 and 9-2 were applied to determine the factored loads. Based on these loads frame USD-2 was designed by the Ultimate Strength Design method using ACI 318-71 provisions. Capacity reduction factor ($\emptyset$) was assumed as 1.0, and the columns were designed such that their capacities were slightly greater than the beam, so the hinges would form in the beam. Beam moment diagram including P-Δ moments, for both loading conditions is shown in Fig. 2.4.
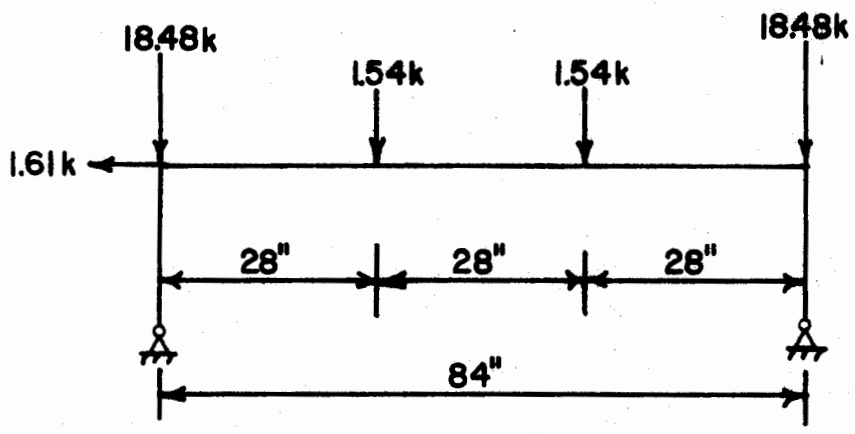
SERVICE LOADS
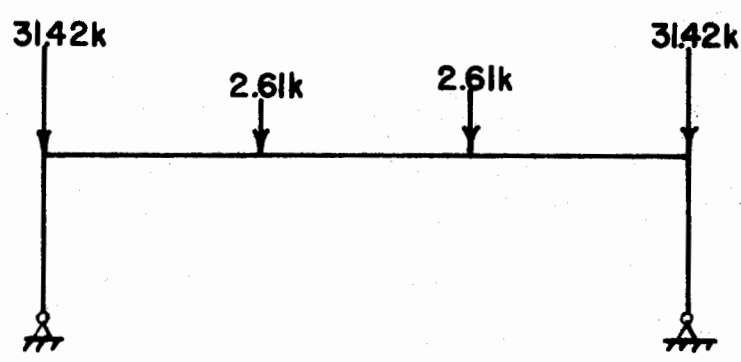
CONDITION I ACI (9-1)
GRAVITY ONLY (1.7 GRAVITY)
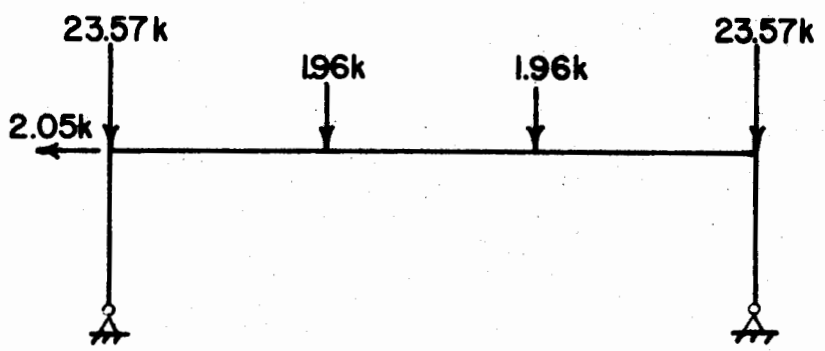
CONDITION II ACI (9-2)
GRAVITY + LATERAL .75 (1.7 GRAVITY + 1.7 W)

Figure 2.3 Service loads and loading conditions
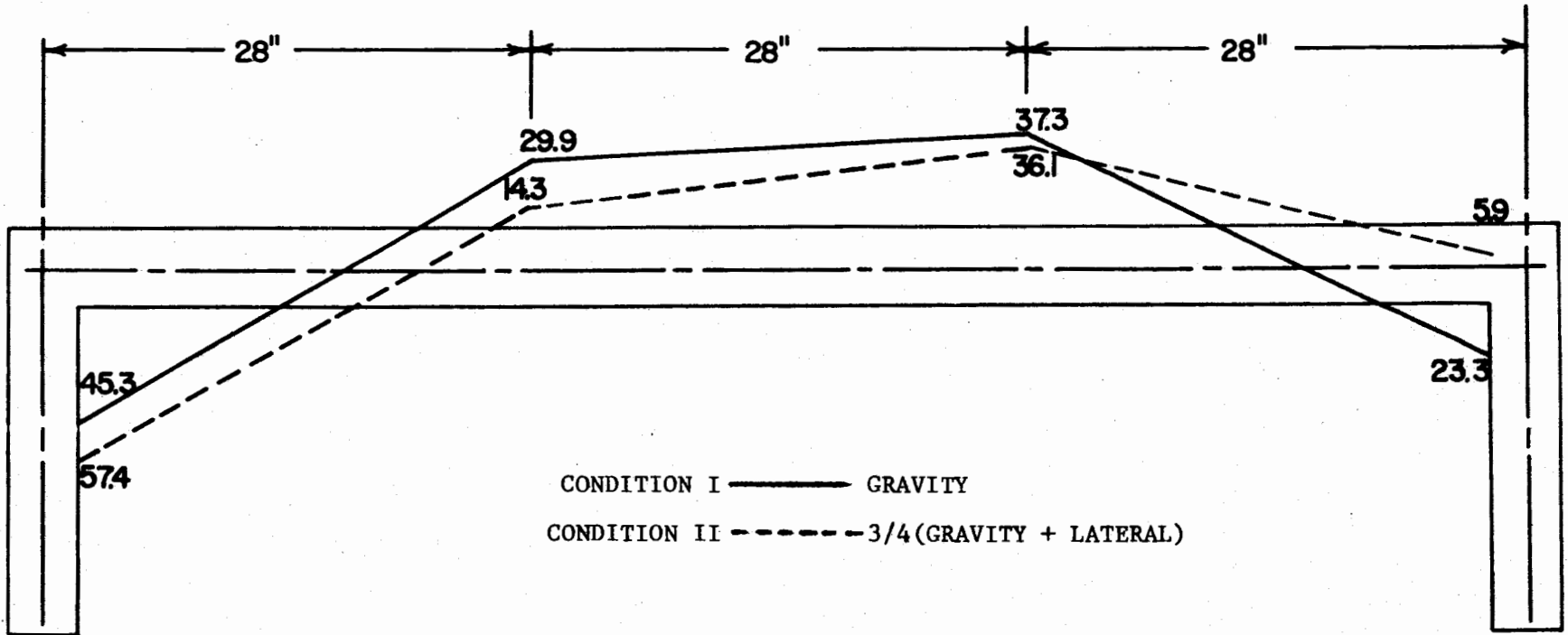
Figure 2.4   Moment diagram, frame USD-2

c) Frame analysis and design of frame USD-2 - Brief design procedure is given below, but a more complete analysis and design of frames may be found in Ref. 11.

Column Design:

   Try   b = 6.00 in   h = 4.00 in   4 #3 bars

       $f_c' = 4000$ psi $f_y = 60.9$ ksi

Condition I (Gravity)

$P_u = 34.03$ k

Column base shear = 1.88 k

@ face $M_u = 18.75" \times 1.88 = 35.3$ k-in

$d' = .105 + .1875 + .4573 = .75$ in

$\gamma = \dfrac{h-2d'}{h} = \dfrac{4.00-(2)(.75)}{4} = .63$

Flexural stiffness of beam and column from P-M-$\emptyset$ plots (not shown):

   $\beta_d = 0$ $EI_c = 51000$ k-in^2

                 $EI_b = 51800$ k-in^2

Determine k:

$\psi_B = \dfrac{EI_c/L_c}{EI_b/L_b} = \dfrac{51000/21}{51800/84} = 3.94$

$\psi_A = \infty$

From Jackson and Moreland's nomograph (12)

K = 3.2

$P_c = \dfrac{\pi^2 EI_c}{(Klu)^2} = \dfrac{\pi^2 \times 51000}{(3.2 \times 18.75)^2} = 139.8$ k

$$\delta = \frac{C_m}{1-P_u/P_c} = \frac{1.0}{1-34.03/139.8} = 1.32$$

$$M_c = \delta M_2 = 1.32 \times 35.6 = 46.6$$

Analysis:

$$\delta e/h = \frac{1.32 \times 46.6}{34.03 \times 4.0} = .452$$

$$m = \frac{f_y}{.85 \ f_c'} = \frac{60.9}{(.85)(4)} = 17.7$$

$$\rho_t m = .0183 \times 17.7 = .324$$

From ACI SP-17A "Ultimate Strength Design Handbook" (13)

Capacity $K = .29$

For $\emptyset = 1$ $K = \frac{.29}{.7} = .41$

Required $K = \frac{P_u}{f_c' bt} = \frac{34.03}{(4)(6)(4)} = .35 < .41$ OK

Condition II (Gravity + Lateral)

$P_u = 26.04$ k

$M_u = 18.75 \times 2.44 = 45.8$ k-in

$EI_c = 49600$ k-in^2

$EI_b = 51800$ k-in^2

$$\psi_B = \frac{EI_c/L_c}{EI_b/L_b} = \frac{49600/21}{51800/84} = 3.83$$

$\psi_A = \infty$

$K = 3.2$

Moment magnifiers (δ):

$$P_c = \frac{\pi^2 EI_c}{(Klu)^2} = \frac{\pi^2 \times 49600}{(3.2 \times 18.75)^2} = 136.00 \text{ k}$$

$$\delta = \frac{C_m}{1 - P_u/P_c} = \frac{1.0}{1 - 26.04/136} = 1.24$$

$$\delta M = 1.24 \times 45.8 = 56.7$$

$$\rho_t m = .324, \quad \delta e/h = .545$$

From ACI SP-17A "Ultimate Strength Design Handbook" (13)

Capacity $\quad K = \frac{.24}{.7} = .34$

Required $\quad K = \frac{P_u}{f_c' bt} = \frac{26.04}{(4)(6)(4)} = .271 < .34 \quad$ OK

Previous trial and errors and P-M-$\emptyset$ plots are not shown.

Beam design:

Draw moment diagram considering joint block statics.

Negative moment @ critical section = 57.4 k-in

Try: b = 6.00"   h = 4.5", $f_c' = 4.00$ ksi, 2 #3 bars

$\quad\quad f_y = 77.3$ kis

Analysis:

d = 3.75 (previous trial & error not shown)

$T = A_s f_y = 2(.11)(77.3) = 17.0$ K

C = T

$.85 f_c' a \times b = 17; \quad a = .833$ in

M = T (d−a/2) = 57.3 k-in   OK

Positive moment @ critical section = 37.3 k-in

Try: b = 6.00"   h = 4.00"   d = 3.43" (after trial & error)

f_c' = 4.00 ksi f_y = 54.1 ksi

Analysis:

$T = A_s f_y$ = (.22)(54.1) = 11.9 k

C = T

.85 f_c' ab = 11.9 k; a = .583 in

M = T (d−a/2) = 37.3 k-in   OK

Check shear:

$v_u = V_u / \emptyset b_w d = \dfrac{2890}{(1.0)(6)(3.79)}$ = 127.1 psi

$v_c = 2\sqrt{f_c'} = 2\sqrt{4000}$ = 126.5 psi

v_s = 127.1 − 126.5 = .60 psi

Use #12 gage wire stirrups @ d/2 = 3.79/2 = 1.90 in spacing. No stirrups required in midspan section.

The envelope moment diagram with detailing of the frame is shown in Fig. 2.5. Complete reinforcing detail of frame USD-2 is presented in Fig. 2.6 and bill of reinforcing is listed in Table 2.1. Cross sectional dimensions of the beam and column are shown in Fig. 2.7.

℄
SYMMETRY

2'-2"

1'-2"

37.3

33.6

14.98"

18.7

10.41"

28.7

a=4.5

57.4

20.81" (P.I.)

ENVELOPE MOMENT DIAGRAM

(1'-3")+1'=2'-3"

1'-3"

4$\frac{1}{2}$"

2'-9$\frac{1}{2}$"

1'-6$\frac{3}{4}$"
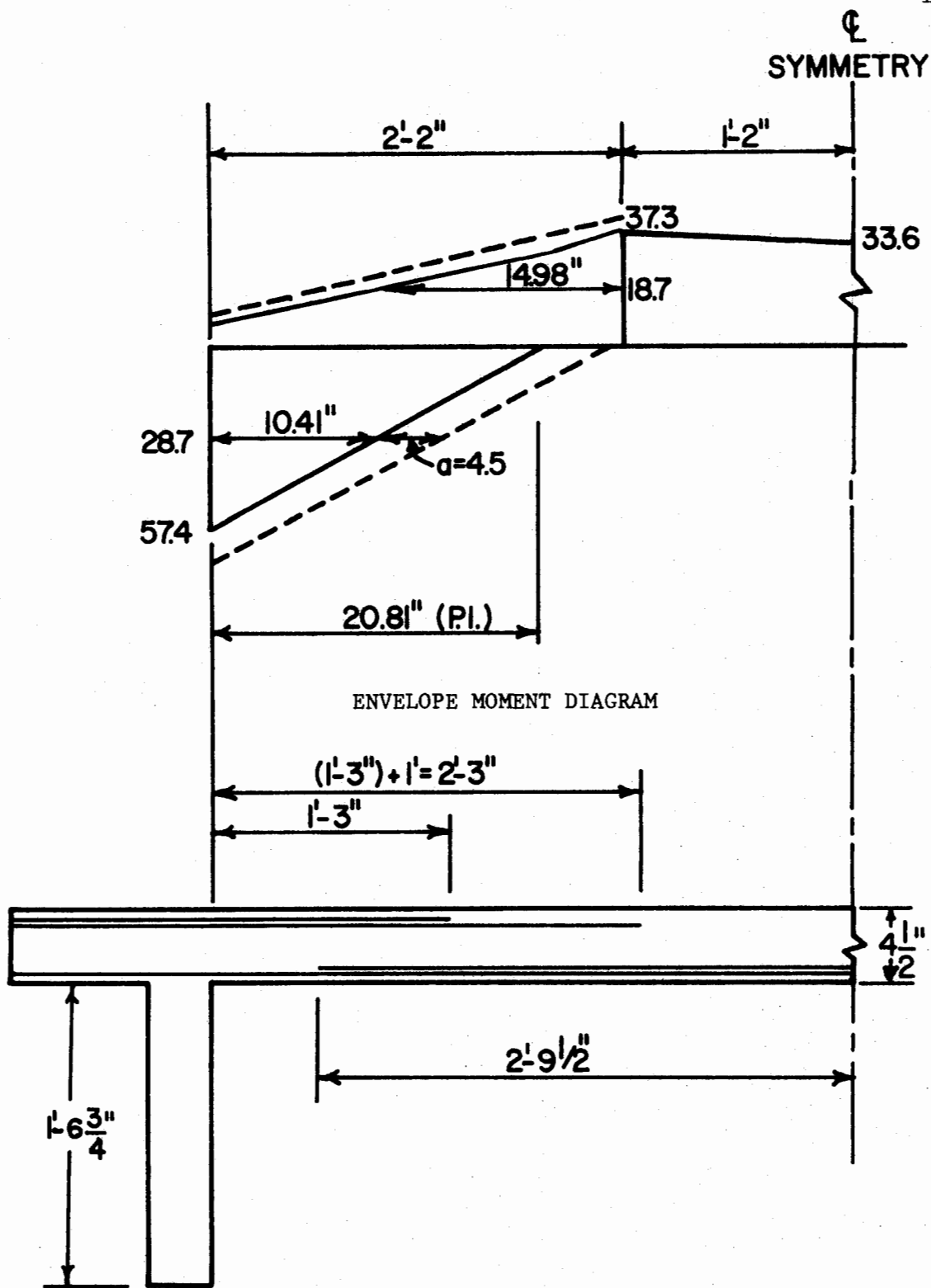
DETAILING OF FRAME USD-2

Figure 2.5   Frame USD-2 detailing
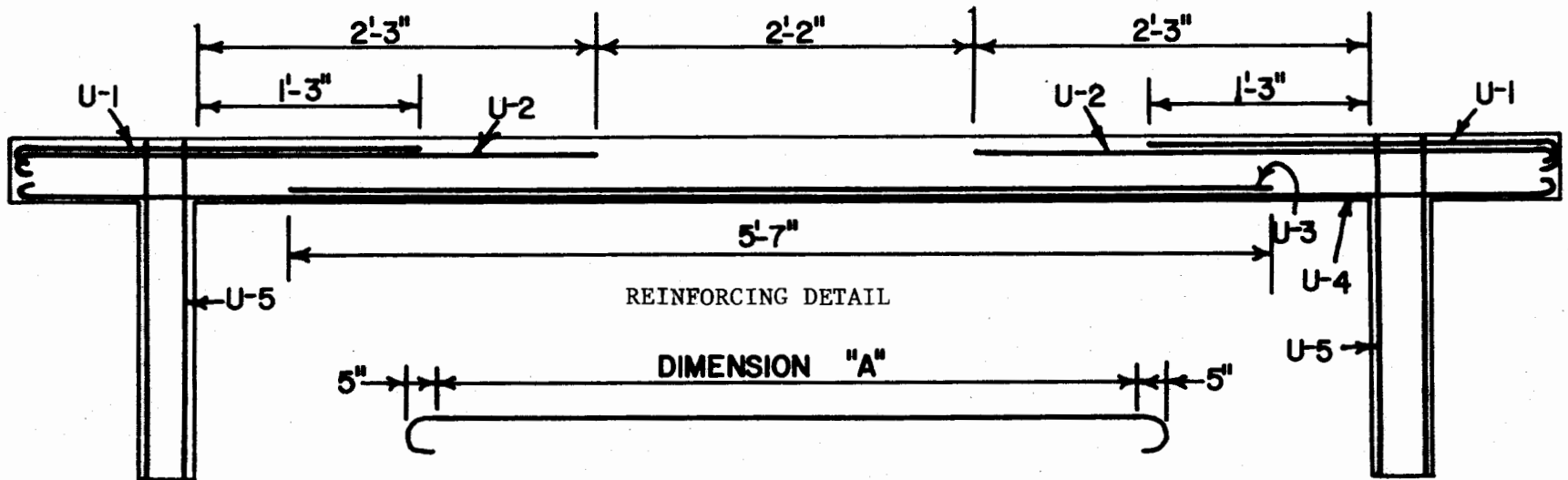
Table 2.1 Bill of reinforcing frame USD-2

BAR	NO. BARS	SIZE	f_y ksi	DIM. "A"	LENGTH
U-1	2	3	77.3	2'-2"	2'-8"
U-2	2	3	77.3	3'-2"	3'-8"
U-3	1	3	54.1	——	5'-7"
U-4	1	3	54.1	8'-6"	9'-6"
U-5	8	3	60.9	——	1'-11¼"

Figure 2.6 Reinforcing detail

a) BEAM CROSS SECTION

.71"

2.72" 4.5"

1.07"

1.625" 2.75" 1.625"

6.00"

$\frac{1}{4}$" $\emptyset$

23.25"

$\frac{1}{2}$" $\emptyset$

c) COLUMN CAGE

.75"

2.5" 4.00"

.75"

1.0" 4.00" 1.0"

6.00"
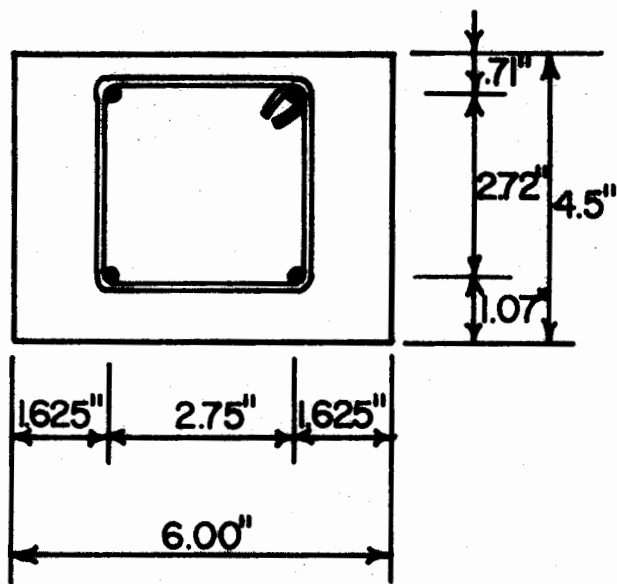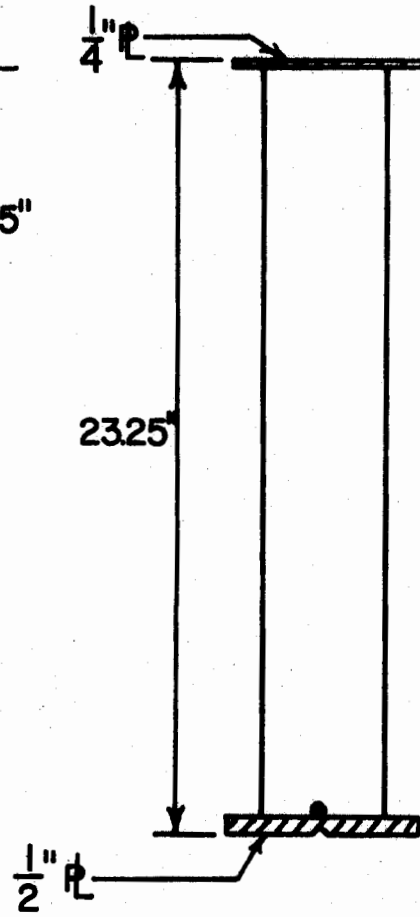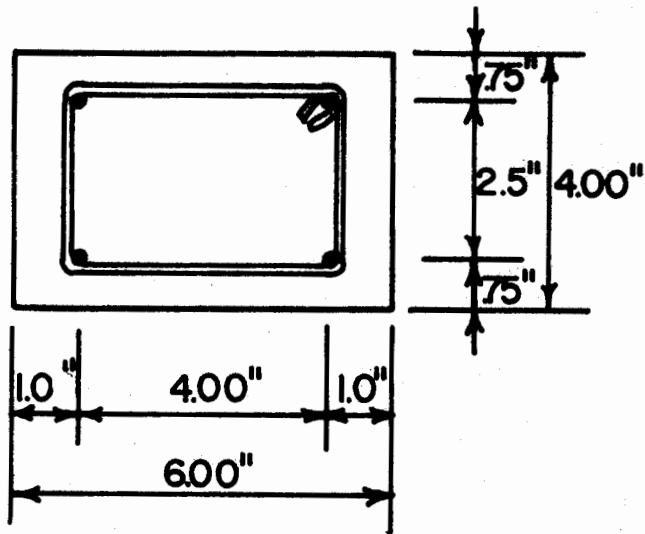
FRAME USD-2

b) COLUMN CROSS SECTION

Figure 2.7 Cross sectional dimensions

d) Frame LD-2 - Frame LD-2 was designed based on the mechanism method. To account for P-Δ moments an estimate of the failure load was determined using Merchant-Rankin formula modified by Wood (14) as: $1/\lambda f = 1/\lambda p + 1/\lambda c$; where λf is the collapse load factor of a partially plastic multi-story structure, λp is the idealized rigid-plastic collapse load factor, and λc is the elastic critical load factor. To achieve a design M_p, the plastic collapse load factor was increased to account for the P-Δ moments. The two loading conditions for the frame LD-2 are shown in Fig. 2.3. The beam moment diagram with P-Δ moment included are drawn for both loading conditions in Fig. 2.8.

e) Frame analysis and design of frame LD-2

Column design:

Try columns   b = 6.00 in   h = 3.75 in   4 #3 bars

$$f_c^{'} = 4000 \text{ psi} \qquad f_y = 59.1 \text{ ksi}$$

Condition I (Gravity)

Flexural stiffness of beam and column from P-M-$\emptyset$ polts (not shown):

$$\beta_d = 0 \quad EI_c = 41900 \text{ k-in}^2$$

$$EI_b = 48700 \text{ k-in}^2$$

Determine K

$$\psi_B = \frac{EI_c/L_c}{EI_b/L_b} = \frac{41900/21}{48700/84} = 3.44$$

$$\psi_A = \infty$$

$$K = 3.0$$
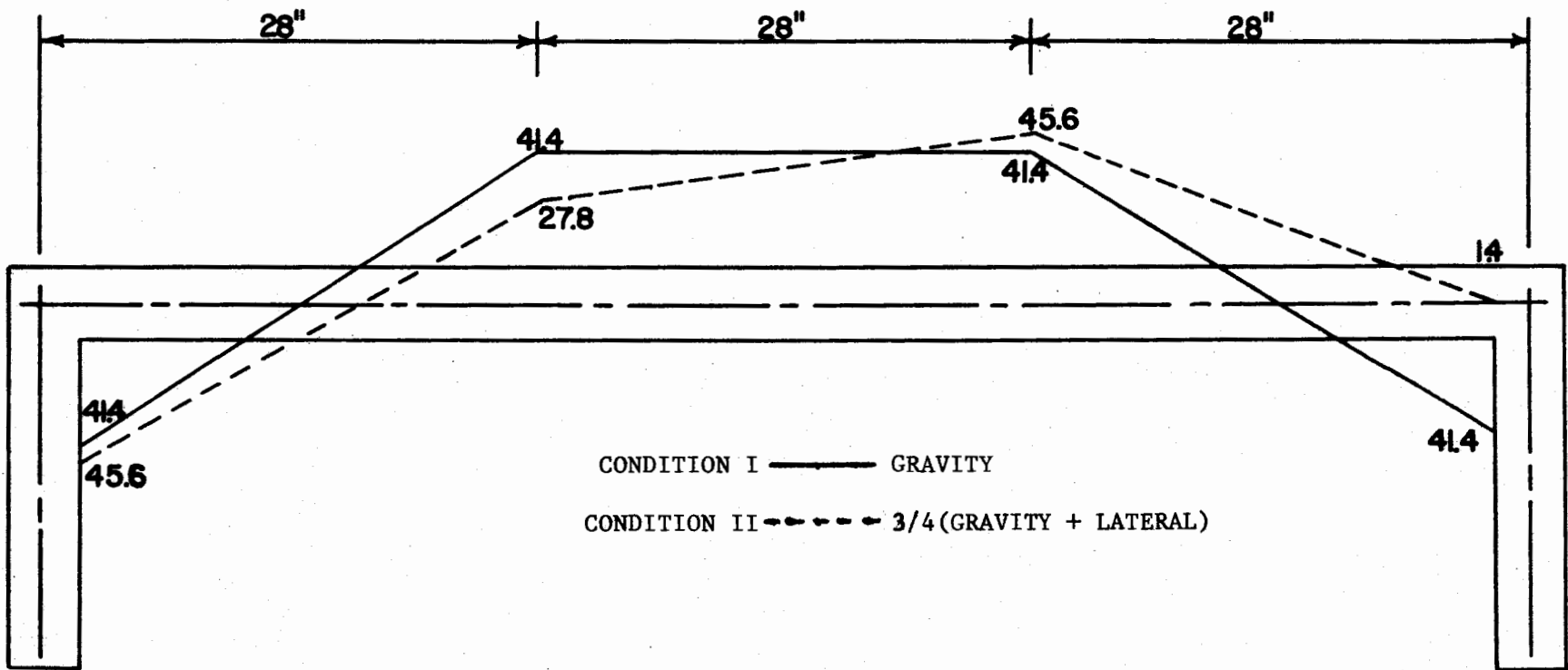
Figure 2.8   Beam moment diagram frame LD-2

$$P_c = \frac{\pi^2 EI_c}{(Klu)^2} = \frac{(\pi)^2(41900)}{(3 \times 18.75)^2} = 130.7 \text{ k}$$

$$\lambda_E = \frac{\text{Critical Load}}{\text{Service Load}}$$

$$\lambda_E = \frac{130.7}{18.48+1.54} = 6.53$$

$$\lambda_P = \frac{.9\lambda_F\lambda_E}{\lambda_E-\lambda_F} = \frac{(.9)(1.7)(6.53)}{6.53 - 1.7} = 2.07$$

Required M_P:

$$M_P = \frac{P_u L_b}{7.77} \text{ from mechanism analysis (not shown)}$$

$$M_P = \frac{(2.07)(18.48)(84)}{77.7}$$

Required $M_P = 41.4$

Equivalent (δ)

$$\delta = \frac{41.4}{34} = 1.22$$

Condition II (Gravity + Lateral)

$$EI_c = 42400 \text{ k-in}^2$$

$$EI_b = 48700 \text{ k-in}^2$$

Determine K

$$\psi_B = \frac{EI_c/L_c}{EI_b/L_b} = \frac{42400/21}{48700/84} = 3.48$$

$$\psi_A = \infty$$

$$K = 3.1$$

$$P_c = \frac{\pi^2 EI}{(Klu)^2} = \frac{\pi^2 \times 42400}{(3.1)(18.75)^2} = 123.9 \text{ k}$$

$$\lambda_E = \frac{\text{Critical Load}}{\text{Service Load}}$$

$$\lambda_E = \frac{123.9}{15.32} = 8.09$$

$$\lambda_P = \frac{.9\lambda_F\lambda_E}{\lambda_E - \lambda_F} = \frac{(.9)(1.7)(8.09)}{8.09 - 1.7} = 1.94$$

Required M_P

$$M_P = \frac{P_u L_b}{49.5} \qquad \text{from mechanism analysis (not shown)}$$

$$M_P = 45.6$$

Equivalent (δ)

$$\delta = \frac{45.6}{40} = 1.14$$

Beam Design:

Required M_p = 45.6 k-in (negative & positive)

Try: b = 6.00 in   h = 4.5 in   2 #3 bars f_c' = 4000 psi

f_y = 60.9

Analysis:

d = 3.73 (previous trial & error not shown)

$T = A_s f_y$

= (2)(.11)(60.9) = 13.4 k

C = T

.85 f_c' ab = 13.4 k

a = 13.4/(.85)(4)(6) = .657 in

M = T(d-a/2)

= 13.4(3/73 - .657/2)

M = 45.6 k-in   ok

Check shear

$\emptyset = 1.0$ $v_u = V_u / \emptyset b_w d$

$v_u = 3170/(1.0)(6)(3.73) = 141.6$ psi

$v_c = 2\sqrt{f_c'} = 2\sqrt{4000} = 126.5$ psi

$v_s = 141.6 - 126.5 = 15.1$ psi

use #12 GA stirrups @ d/2 = 3.73/2 = 1.87 in.

No stirrups required in mid span region

Detailing of the frame is shown in Fig. 2.9. Table 2.2 shows the bill of reinforcing and the complete reinforcing detail is shown in Fig. 2.10. Nominal cross sections for beam and column are shown in Fig. 2.11.
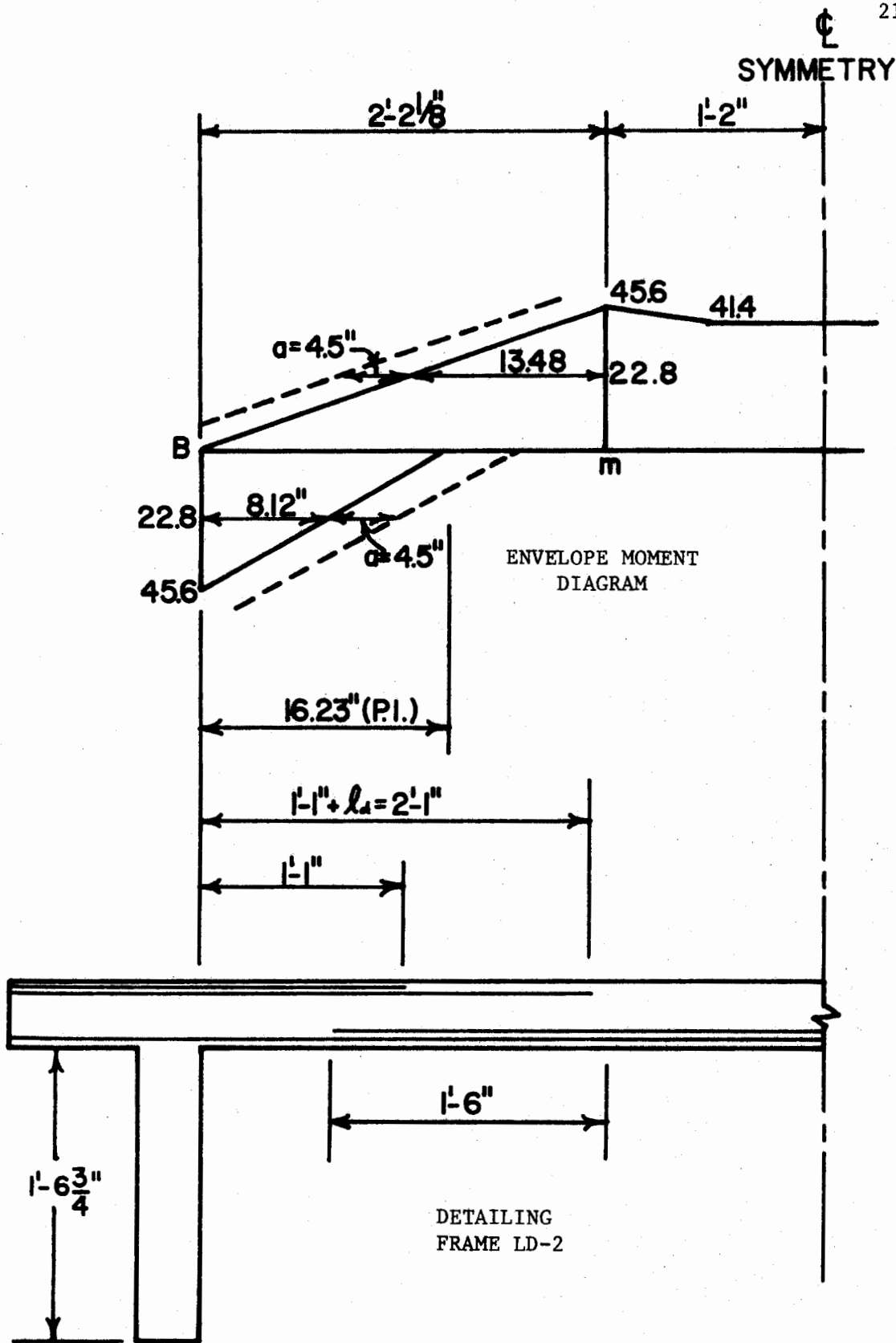
Figure 2.9   Frame LD-2 detailing

REINFORCING DETAIL
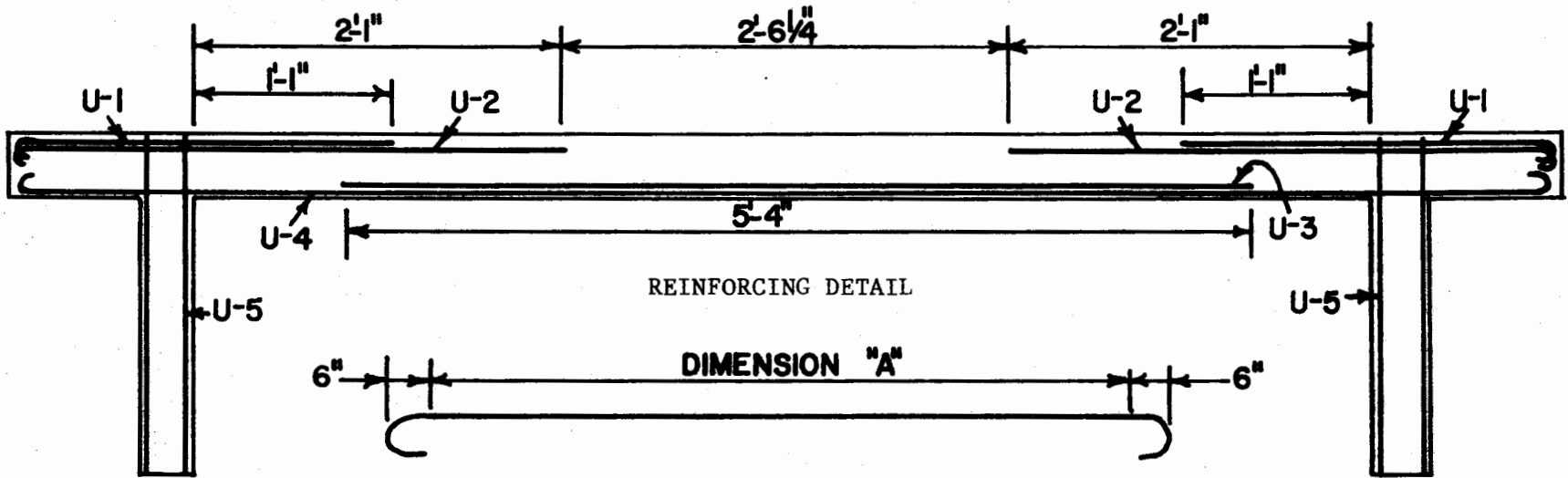
DIMENSION "A"

Table 2.2 Bill of reinforcing frame LD-2

BAR	NO.BARS	SIZE	fy ksi	DIM. "A"	LENGTH
U-1	2	3	60.9	2'-0"	2'-6"
U-2	2	3	60.9	3'-0"	3'-6"
U-3	1	3	60.9	———	5'-4"
U-4	1	3	60.9	8'-6"	9'-6"
U-5	8	3	59.1	———	1'-11¼"

Figure 2.10 Reinforcing detail frame LD-2

BEAM CROSS SECTION

.71"
272" 4.5"
107"

1.625" 2.75" 1.625"

6.00"

COLUMN CROSS SECTION

.75"
2.25" 3.75"
.75"

1.0" 4.00" 1.0"

6.00"

1/4" ℟

23.25"

1/2" ℟

COLUMN GAGE

V-NOTCH
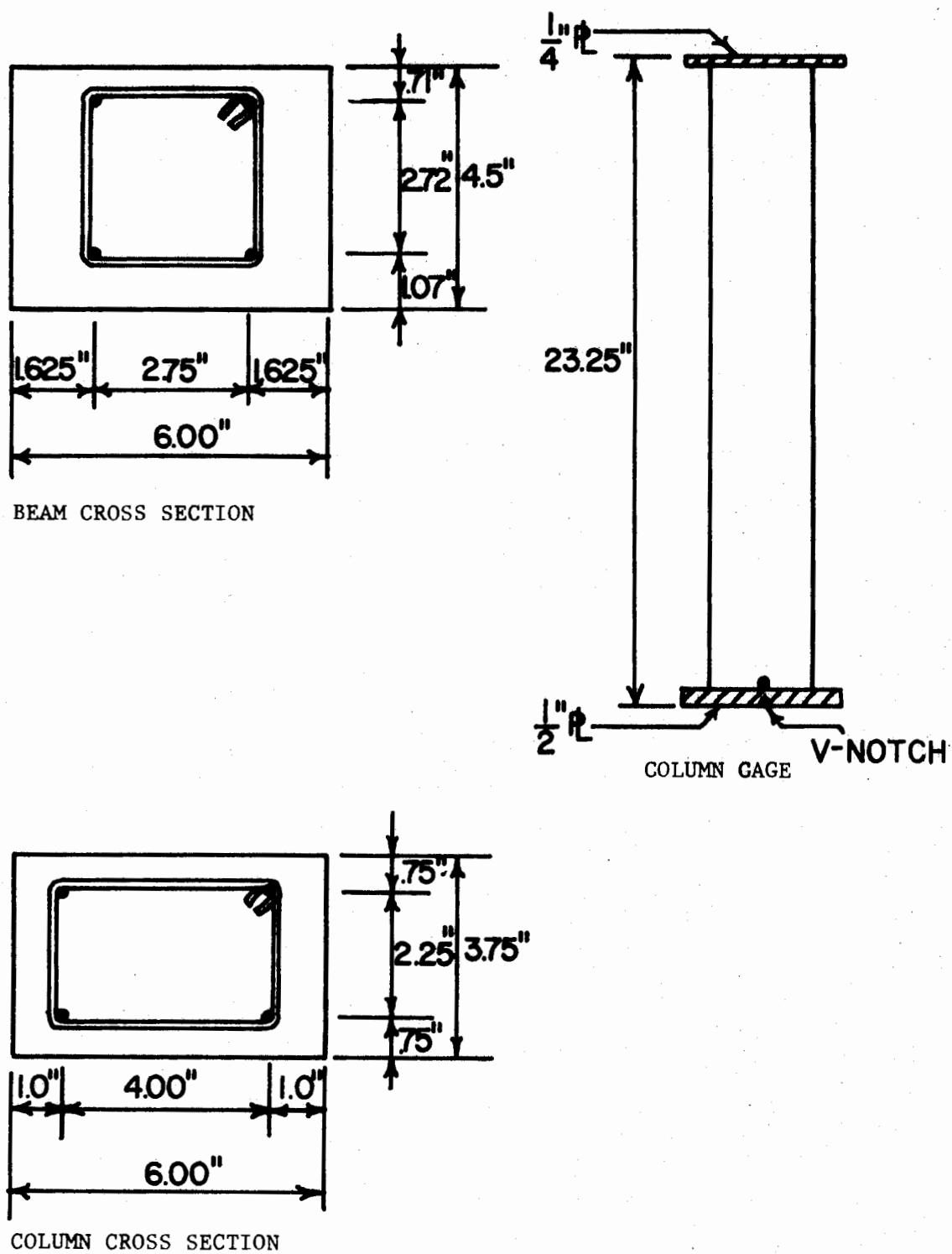
Figure 2.11 Cross sectional dimensions of beam and column

CHAPTER III

PHYSICAL TESTS

3.1 GENERAL

As the experimental part of this investigation two frames, designated as USD-2 and LD-2 were prepared and tested to failure with short time loading in horizontal position. Frames USD-2 and LD-2 are shown schematically in Fig. 3.1. These frames were symmetrical with respect to the vertical axis through beam mid-span. The load components are shown in Fig. 3.2. Preparation of the specimens, instrumentation, loading and testing were done in the concrete laboratory, Portland State University.

3.2 PRINCIPAL PROPERTIES OF FRAMES

The principal properties of the two frames, measured after frames were cast, are listed in Table 3.1. The quantity ρ_t is defined as the total reinforcement/gross area.

TABLE 3.1 PRINCIPLE PROPERTIES OF THE FRAME

	Member	t in	b in	ρ_t	f_c' psi	f_y ksi
FRAME USD-2	AB	3.986	6.044	.01826	4607	59.1
	BC	4.514	6.063	see detail	4498	77.3
	CD	3.994	6.002	.01835	4607	59.1
FRAME LD-2	AB	3.731	6.054	.01948	4372	59.1
	BC	4.488	6.057	see detail	4645	60.9
	CD	3.745	6.023	.01950	4372	59.1

(a) TEST FRAME USD-2
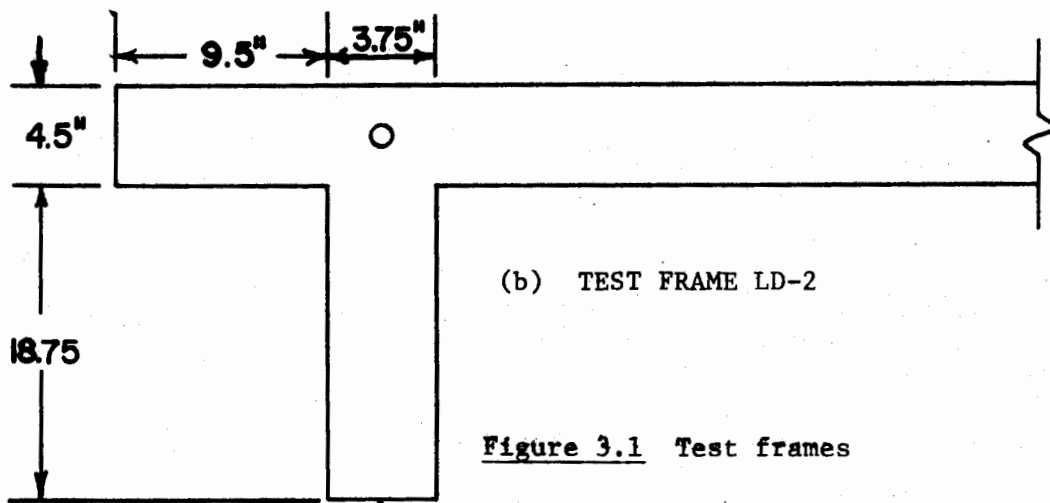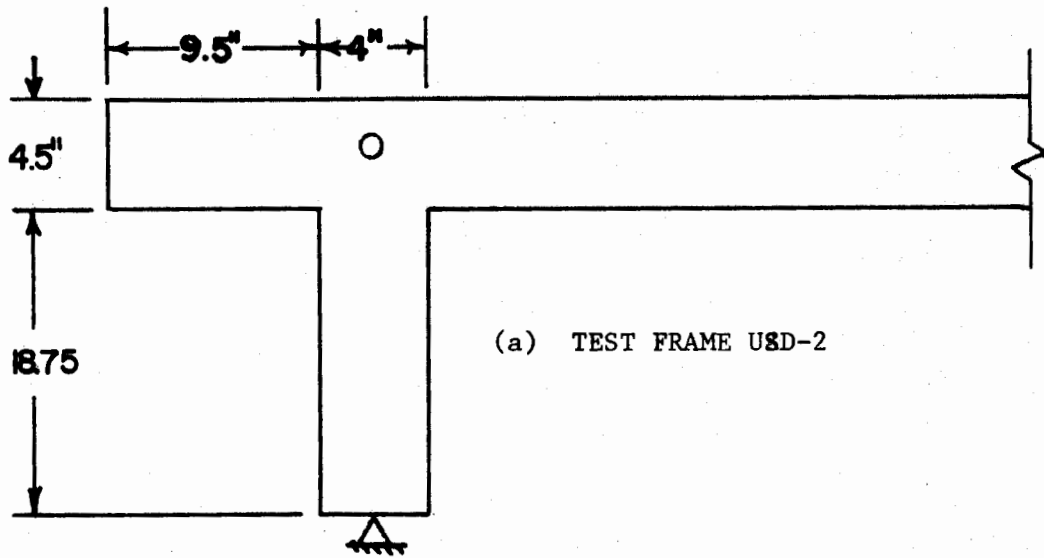
(b) TEST FRAME LD-2

Figure 3.1 Test frames
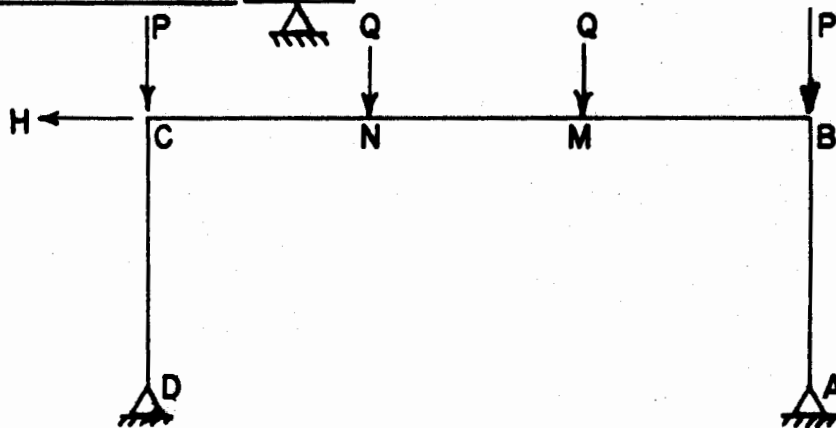
Figure 3.2 Load components of test frames

3.3 MATERIALS

a) Reinforcing steel – different sizes of intermediate grade steel were used in the frames. The reinforcing bars in all columns and beams were #3 bars. The tension yield strength of the reinforcing steel was obtained from test coupons which were cut from bar stocks and tested by the Material Testing System hydraulic machine at Portland State University

b) Concrete – the concrete mixture was designed to provide an average compressive strength of 4000 psi at six days. The cement used was Type III (high early strength), the fine aggregate was Willamette River basin sand and the coarse aggregate was graded pea gravel of 3/8 in. maximum size.

3.4 SPECIMEN FORMWORK

The forms used consisted of 10 inch steel channels welded together, used as the base, and 6-inch steel channels for the sides. Base channels were laid on 2 x 4 lumber grillage and were levelled in both directions using a hand level. Raising the forms by 2 x 4 sections facilitated erection and removal of the side channels. The center line of the frame was scribe marked on the base channels and accurate dimensions of the frame at the base were maintained by adjusting the position of the side channels. In order to adjust the side channel to proper positions, 18 pieces of 4 inch angles were welded to the base channels at frequent intervals. A bolt was welded to side channels at these intervals and through a drilled hold in angles with two nuts at each side. Proper dimensions at the top surface were then maintained by adjusting the

positions of the nuts. Schematic diagram and a photograph of the forms are shown in Fig. 3.3 and 3.4.

3.5   SPECIMEN FABRICATION, DETAILS, CASTING AND CURING

Both frames USD-2 and LD-2 were reinforced with #3 bars. Nominal cross sections of the beams and columns are shown in Fig. 2.7 and 2.11. Both frames had a beam cross section of 6.00 in. wide by 4.5 in. deep. Columns in frame USD-2 were 4.00 in. deep by 6 in. wide, and frame LD-2 columns were 3.75 in. deep by 6.00 in. wide.

A typical column cage contained two plates at top and bottom with planar dimensions same as column cross sections. Reinforcing bars were welded to these plates at predrilled hold location and reinforcing bars were tied by #12 gage wire ties and 4.00 in. intervals. Fig. 3.5 shows a typical column cage.

For assembling the beam cage, rebars were cut allowing 10.00 in. at one end, and bent into a 180° hook using a bar bending jig. The one continuous bar in each beam was hooked at both ends. Beam cages were assembled by placing the bars on wooden supports, and tied with #12 gage wire stirrups at 1.9 inch intervals where stirrups were required by design. Fig. 3.6 shows a typical beam cage.

To obtain the same concrete cover as in design, small steel chairs were tied to the beam cage on three faces, at frequent intervals. Once the cages were ready the form was oiled and cages were placed in the form. A 7/8 in. (O.D.) x 6 in. steel pipe was inserted through the cage and the base channel at the intersection of beam and leeward column center lines. This pipe was used for application of the lateral load. Concrete was then poured to the level of the form and a small vibrator
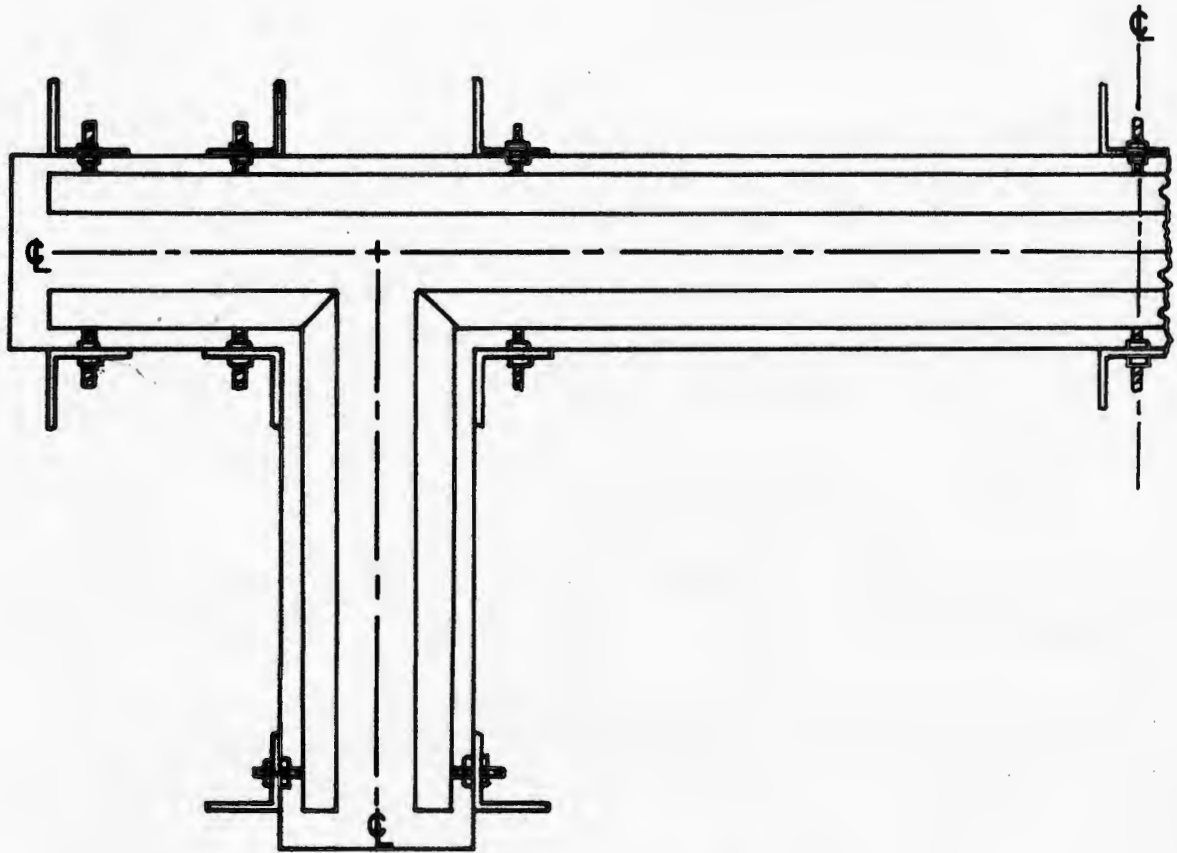
Figure 3.3. Schematic diagram of the form

Figure 3.4. Form preparation before placing beam and column cages

Figure 3.5. Column cage assembly
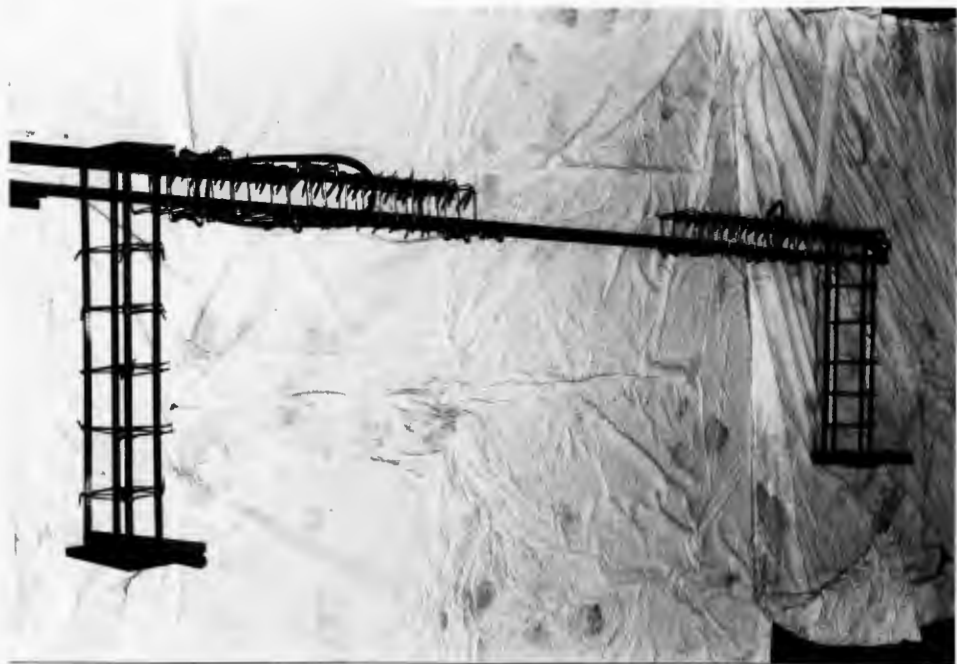
Figure 3.6. Beam cage assembly

was used while casting. Concrete on top was screeded and then covered
with damp burlap.

Twenty-four hours later the form was removed and the frame was
lifted and placed over water saturated curing mats where the frame was
cured wet for about four days; then lifted and transferred to the test
bed and prepared for measurement and instrumentation. Table 3.2 shows
the overall geometrical dimensions of each frame as measured after
casting.

3.6 INSTRUMENTATION
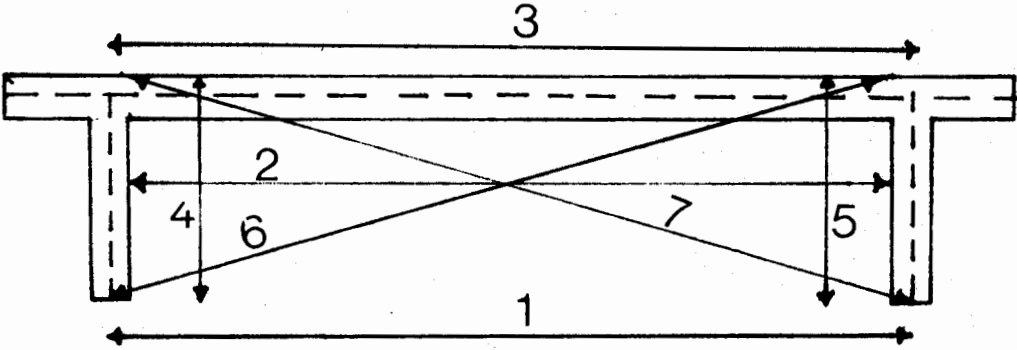
a) General - In the experimental frame tests the following
measurements were taken:

1) Column axial loads P, Beam loads Q and sway load H

2) Lateral deflection

3) Concrete surface strains at various stations (to estimate
   the bending moment at mid point of each station).

b) Loading instrumentation - A loading sequence consistent with
the ACI 318-71 building code (10) requires that lateral loads should be
applied on 75 percent of the vertical loads. Thus the column and
beam loads were incrementally applied, until the design gravity loads
were reached. The lateral load was then applied until frame failure.

The system used for the application of the column loads con-
sisted of 30 ton capacity hydraulic rams and a pump equipped with pre-
ssure gages in range of 0-10000 psi. Since the column axial loads were
the same for both columns, pressure hoses from the column rams were
connected to a manifold, and only one pump was used to apply both
column loads.

TABLE 3.2   MEASURED OVERALL GEOMETRY OF FRAMES

	1	2	3	4	5	6	7
FRAME USD-2							
ACTUAL	84.031	84.031	84.031	23.1875	23.250	85.250	85.281
IDEAL	84.000	84.000	84.000	23.2500	23.250	85.232	85.232
FRAME LD-2							
ACTUAL	84.031	84.031	84.0625	23.250	23.250	84.438	85.375
IDEAL	84.000	84.000	84.000	23.250	23.250	85.353	85.353

Beam loads (Q) were applied using a 20 ton hydraulic ram and lateral load was applied by a 12-ton ram. Column loads, beam loads and lateral load devices are described in section 3.7 c, d and e.

All gravity loads were measured by 10,000 psi capacity pressure transducers. The lateral load was measured using a 10-kip capacity load cell, and monitored by pressure transducer. Pressure transducers and load cell were calibrated using MTS hydraulic testing machine.

c) Concrete strain measurements - Curvature meters were used for measuring concrete surface strains at different stations along the members. Average curvatures were determined by summing the changes in dial readings on two sides and dividing it by the transverse distance between dials.

The schematic diagram of curvature meters are shown in Fig. 3.7. Positions of curvature meters on the frame are shown in Fig. 3.8 and a photograph of curvature meters is shown in Fig. 3.9.

d) Corner rotation measurements - Angular rotations were measured at corners A and D by using a dial gage system shown in Fig. 3.10. This system consisted of a $3/4\emptyset$ x 9 in. long steel solid bar welded at center of base plates of the column cages cast in concrete; and a 1 x 1 x 18 in. angle (arm) welded to a 1 in $\emptyset$ (O.D.) x 3 in. pipe that slipped over the $3/4\emptyset$ solid bar, as shown in Fig. 3.10.

Rotation of the arm was measured by a one inch travel dial gage (LC-8) and by applying the relationship $\theta = \Delta(D.R.)/L$ (where $\Delta D.R.$ is the change in dial reading, and L is the length from center of the pipe to the point of contact of dial gage). This system is applicable
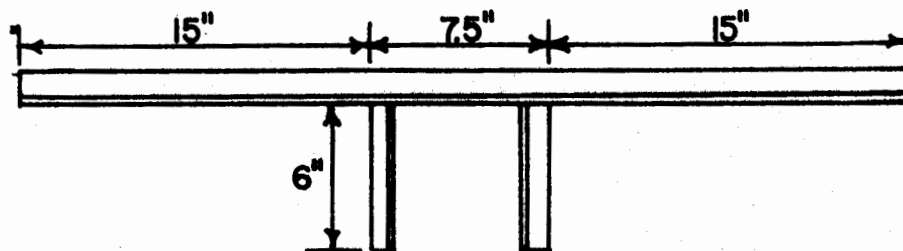
(a)   COLUMN CURVATURE METER
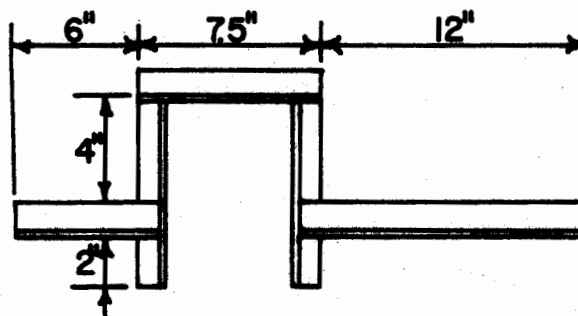
(b)   BEAM CURVATURE METER AT CENTER
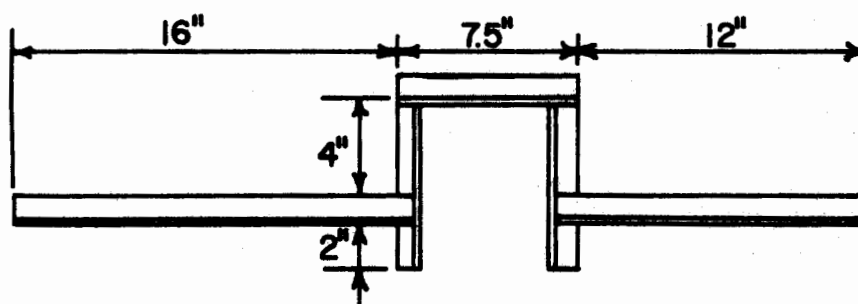
(c)   BEAM CURVATURE METER AT CORNER B & C

Figure 3.7.   Beam and column curvature meters
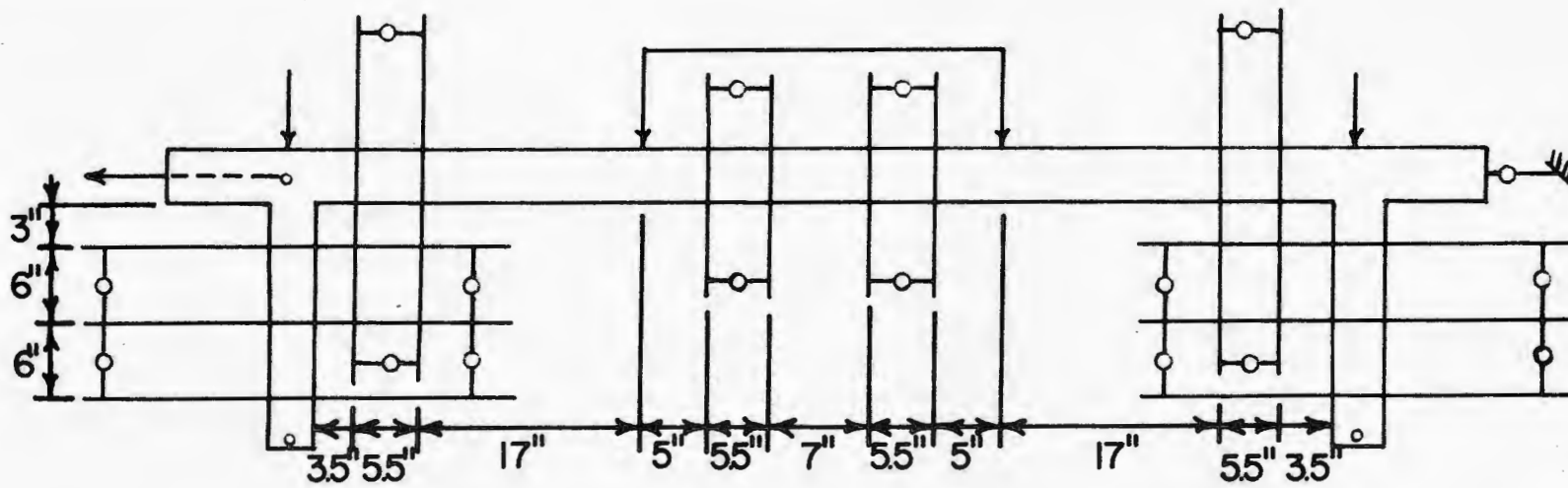
Figure 3.8. Location of curvature meters, rotation dials and lateral deflection dial
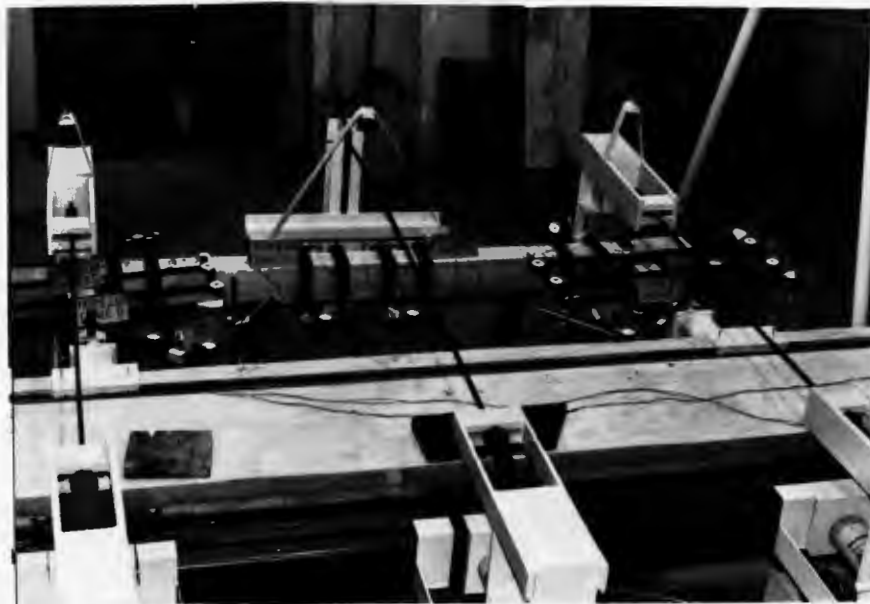
Figure 3.9. Curvature meters in position
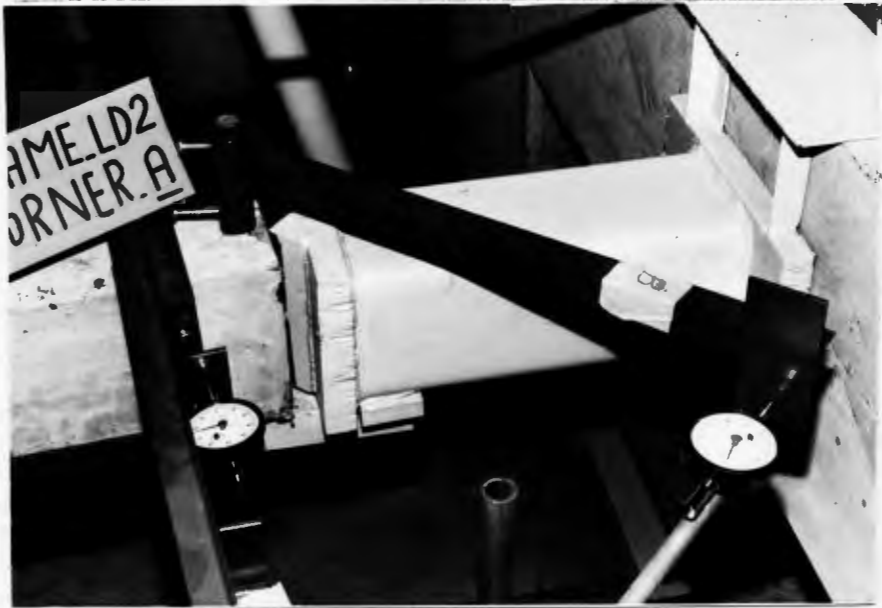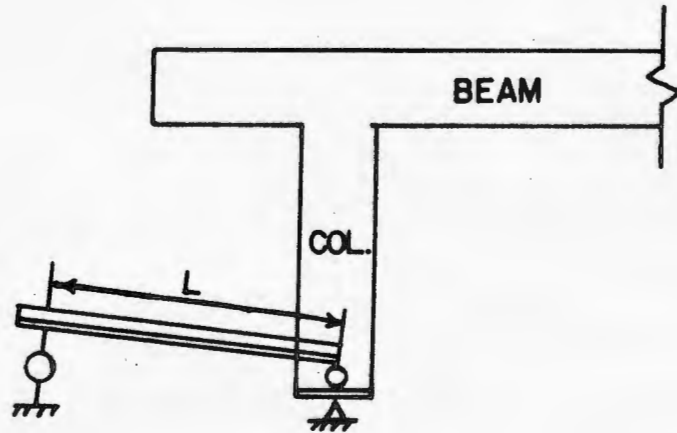
Figure 3.10. Corner rotation measurement system

only for corners that rotate without translation.

e) Lateral deflection measurement - Lateral deflection of the
frame was measured at corner B, using a 2-inch travel dial gage
(LC-10). Dial gage was attached to a pipe cast in a concrete block
as shown in Fig. 3.11. Since frames were symmetrical with respect to
both the loading and geometry no lateral deflection under gravity
loads was theoretically expected. In actual testing, there were slight
lateral deflections, which could be due to imperfection of both frame
geometry and the loading system.

3.7   LOADING SYSTEM COMPONENTS

a) General - The general test set up as shown schematically in
Fig. 3.12 basically consists of a concrete reaction beam (A), movable
steel load beam (b), bearing heads and column heads. The detail of
concrete reaction beam is shown in Fig. 3.13. Movable steel loading
beam (B) is a 12-ft long structural steel tubing TS 1/4 x 6 x 6
resting on wheels which bear against the concrete reaction beam
through a set of roller nests. Three steel plates 1/2" x 6" x 14"
welded to steel tubing at location of roller nests provide extra
stiffness at these locations. Roller nests allow the steel beam to
move laterally, so the ram axes (strands) remain parallel to the original
column center lines during testing. An overall view of test set up is
shown in Fig. 3.14. As shown in Fig. 3.15 and the schematic diagram on
Fig. 3.16, each roller nest is fabricated by four 2"∅ x 8" long solid
bars connected to two steel angles by 1/2"∅ pins through ball bearings
on top and bottom. Roller nests are suspended from a steel angle welded
on top of steel beam (B) when no load is applied. During loading

SEP • 76

Figure 3.11. Lateral deflection measuring device
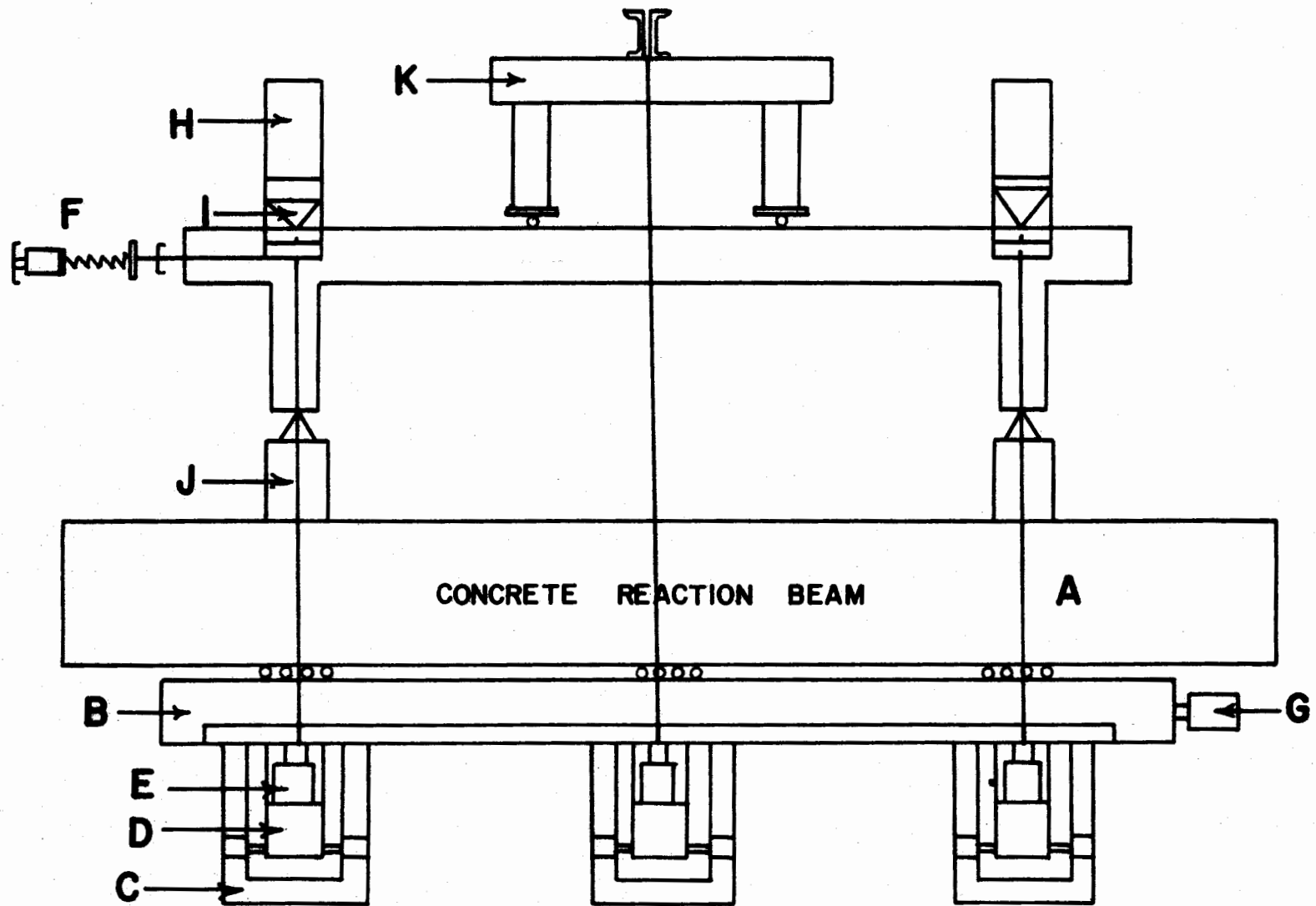
Figure 3.12. Schematic diagram of frame and loading system

ELEVATION

2'-6"   1'-0"

1'-6"
C3"x4½"x10"
5'-6"

SECTION 1

#4 STIRRUPS
3#9 BARS
1.5"COVER
℄ 1½"x6"x10"
WITH ¾"∅ STUDS
2"
COVER
1'-2"
2'-0"

SECTION 2

3½"COVER
8#8BAR
1½"COVER
2'-0"
1'-6"
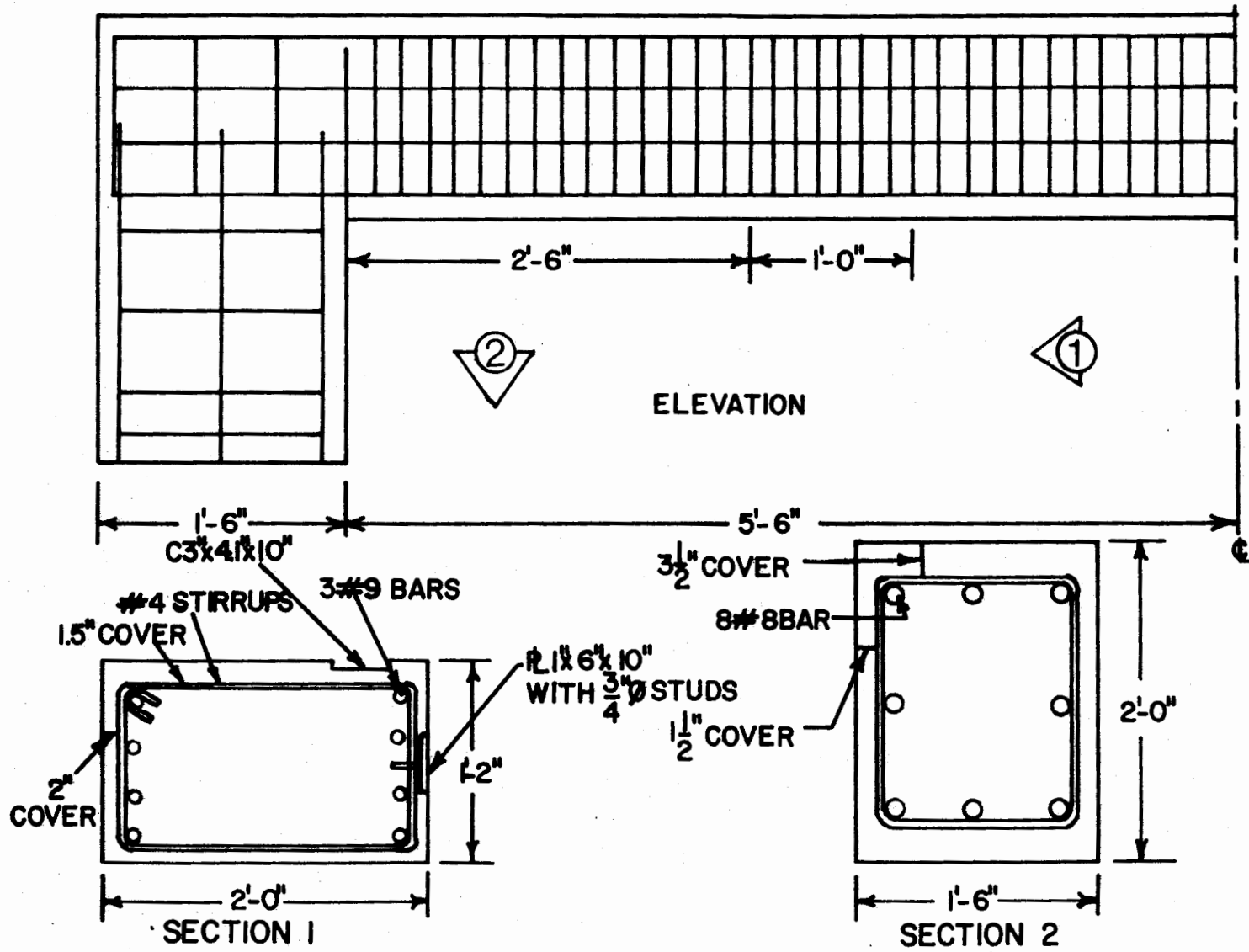
Figure 3.13. Detail of concrete reaction beam
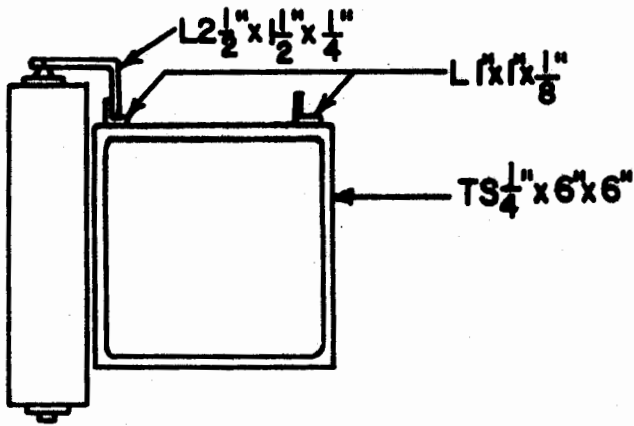
a) CONNECTION OF MOVABLE STEEL BEAM AND ROLLER NEST
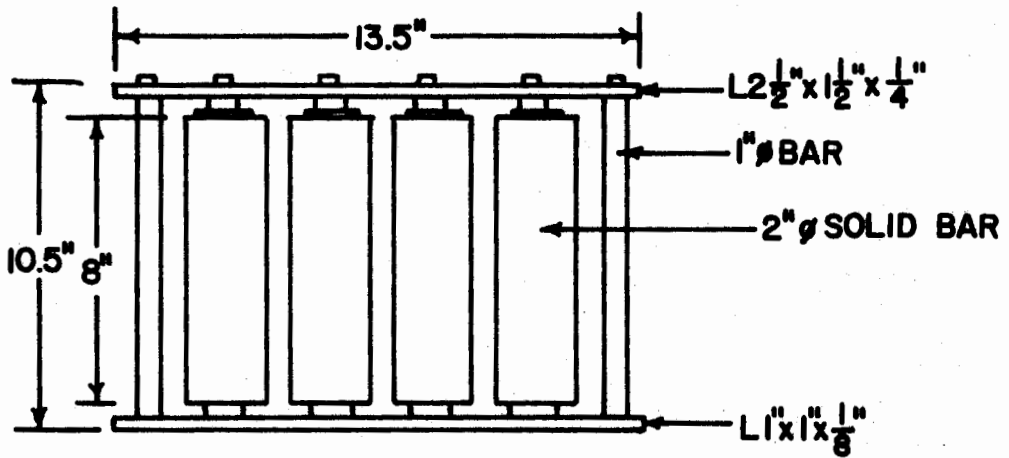
b) DETAIL OF ROLLER NEST
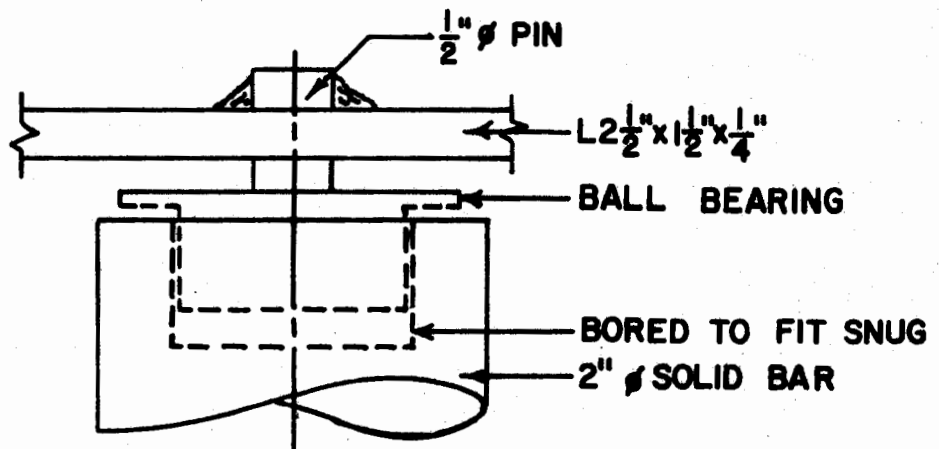
c) END DET.

Figure 3.16. Roller nest system

relative displacement of steel beam and roller nests is free to occur.

b) Reaction devices and sway adjustment system - Reaction device (J) was designed to transfer the loads from column to concrete reaction beam. A reaction device is shown in Fig. 3.17. The reaction device was suspended from concrete reaction beam.

The direction of the column load was one of the most influential components of the loading system on the frame response. The direction of column axial loads were set by aligning the column load strands using a transit. Since this condition must remain during testing, a sway adjustment system (G) was designed to move the steel beam (B) a distance equal to the lateral deflection. As shown in Fig. 3.18, it consists of a ram operated by a pump. The ram is attached to an I-beam that is securely bolted to the concrete slab.

c) Column load devices - Bearing head (D) is designed for a maximum load of 200 kips. As shown in the schematic diagram of Fig. 3.19, it consists of a section of S 12 x 31.8 with four PL 3/4" x 5" x 28" welded on both sides at top and bottom. A 30-kips capacity ram is mounted at center of the flange. With wheels on both sides, the bearing head is able to move in a direction perpendicular to steel beam (B). A photograph of a column bearing head is shown in Fig. 3.20.

Column heads (H), shown in Fig. 3.21, were built similar to bearing heads. A point loading hinge was made by cutting a triangular piece from a PL 2" x 4" x 7". This piece was welded to the web at mid height of column heads. For each column the bearing head was interconnected to the column head by two 1/2"∅ 270K strands at top and bottom. Bearing heads rest on steel frames (C). The schematic diagram of wheel

Figure 3.17   The reaction device

Figure 3.18.   Sway adjustment system

$⅃\frac{1}{4}"x2\frac{1}{4}6"$

$\frac{3}{4}"∅\,SOLID\,BAR$

$⅃\,I"x8"x8.5"$

$SI2"x31.8"$

$⅃\frac{3}{4}"x5"x28"$
ON EACH SIDE

$\frac{1}{2}"∅\,STRAND$

5"

12"

18"

30.5"

a)   ELEVATION VIEW

$⅃\,I"x\,3"x5"$

ADJUSTMENT NUT

CHUCK

RAM

$⅃\frac{3}{4}"x5"x28"$

$⅃\,I"x8"x8.5"$

STIFFENER $⅃$

SI2x31.8

3"

7"

12"

28"

6.5"
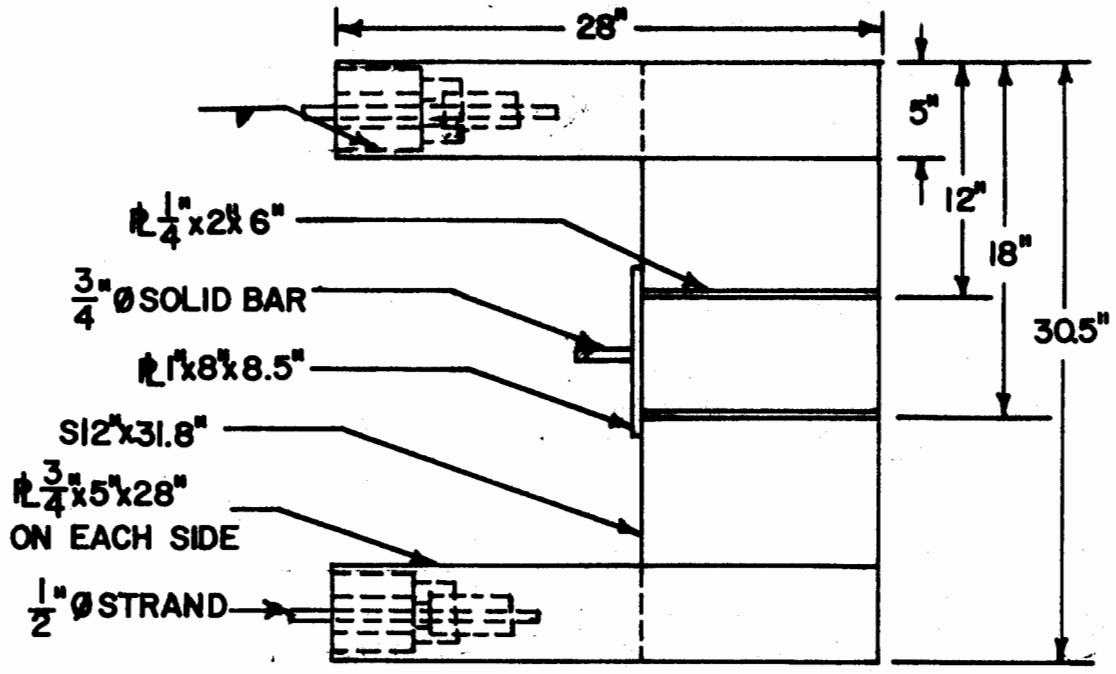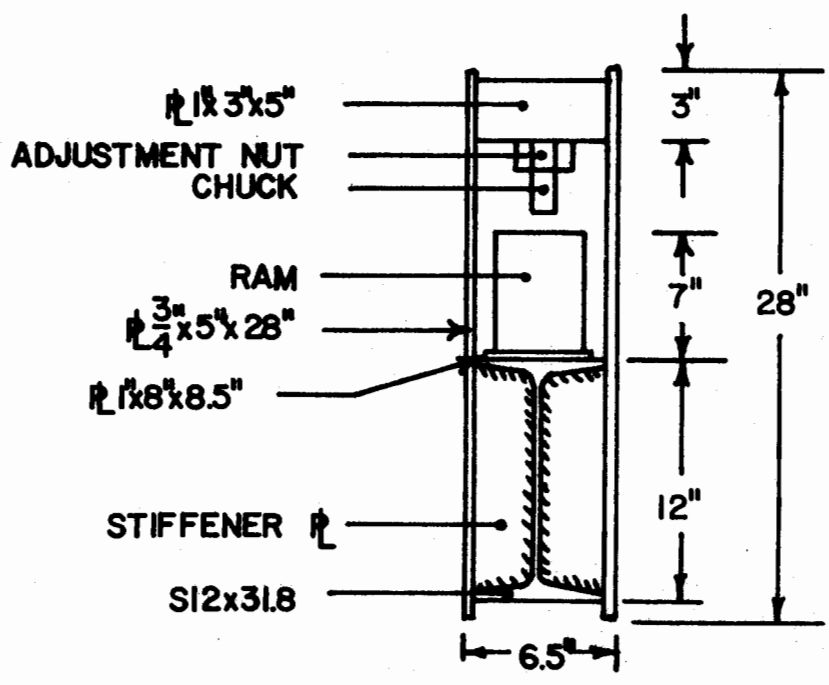
b)   TOP VIEW

Figure 3.19. Bearing head
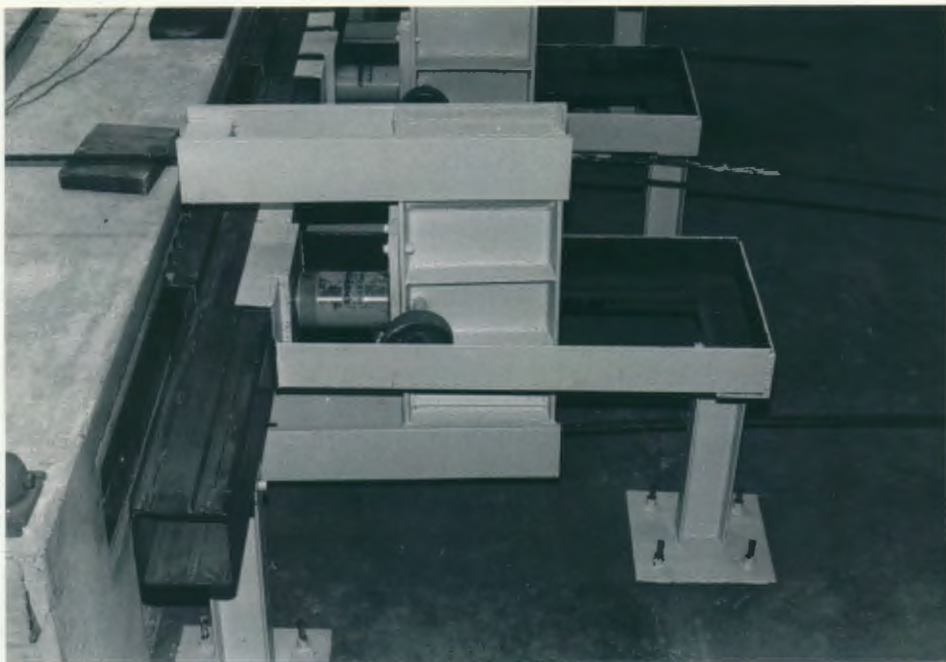
Figure 3.20. Column bearing head

Figure 3.21. Column head

stand which supports the steel frame (C) is shown in Fig. 3.22.
Column heads were suspended from trolleys which were free to move along
a level steel track, made of a S 4 x 7.7 x 12 feet long, 9'-8" high
above the floor. The overall dimensions of this support frame is
shown in Fig. 3.23. Fig. 3.24 shows the trolley and tubular column
supports of the suspension system.

d) Beam load device - The system used for applying the beam
loads consisted of a bearing head similar to those used for column
loads, and a beam head (K) connected to the bearing head by two 1/2"∅
strands at top and bottom. The beam bearing head was designed for a
maximum load of 120 kips.

As shown in schematic diagram of Fig. 3.25a the beam head
consisted of two C 6 x 8.2 x 32" long standing vertically, back to
back, one inch apart, and welded at midheight to two C 6 x 8.2 x 32"
long back to back, 1/2 inch apart. The beam head was suspended from
the same track used for column heads. Fig. 3.25b shows the suspended
beam head.

e) Lateral load system - The lateral load system used for applying
the horizontal load H was designed such that it would have sufficient
strength and displacement capacity. To accomplish this purpose the
following mechanism was used: A 3/4-in. diam. steel bar was inserted
through the pipe cast at corner C. Two 1/4"∅ bars connected this 3/4-in
bar to a steel channel section, as shown in schematic diagram of Fig.
3.26(a). A 1/2"∅ steel bar connected to the center of this channel
and ran through a steel angle and a spring system which helps maintain
the lateral load while the test specimen is creeping. The bar was
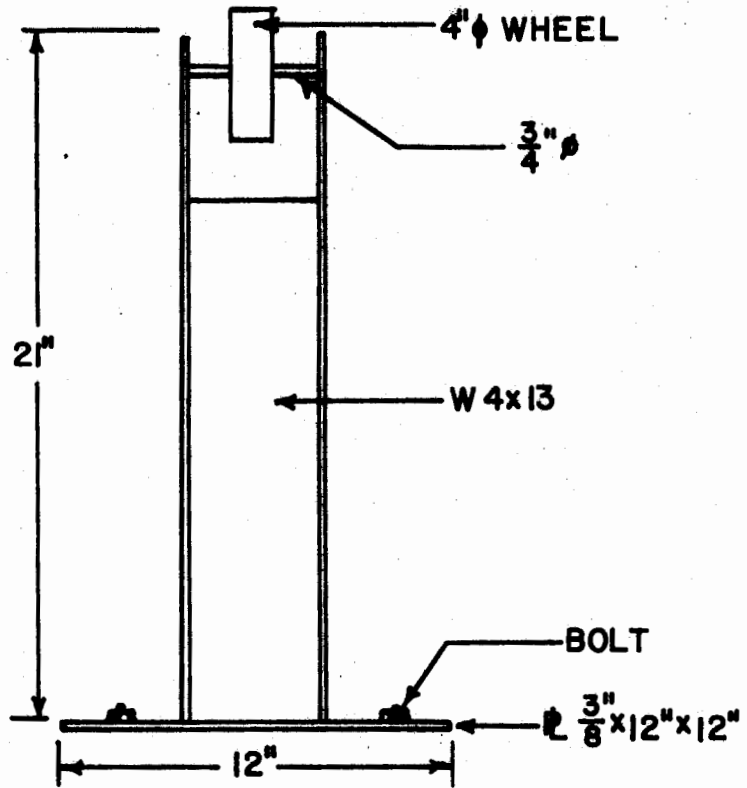
Figure 3.22   Detail of wheel stand
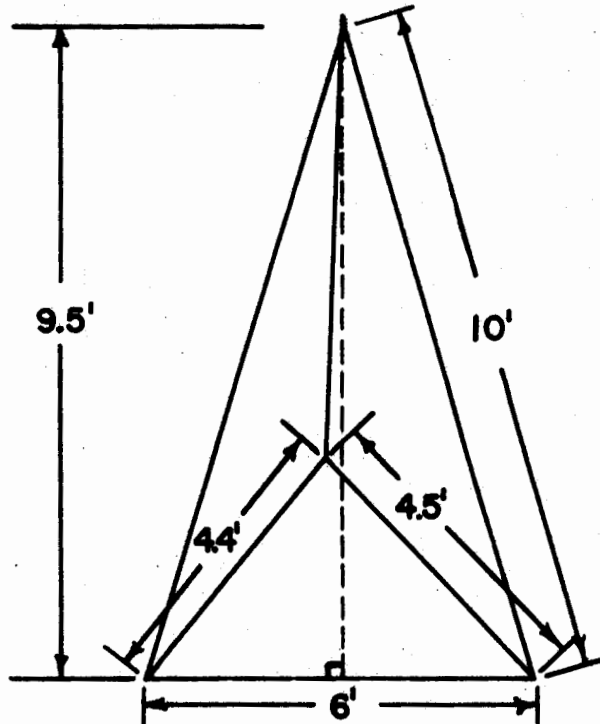
Figure 3.23   Elevation diagram of support frame

a) TROLLEY

b) SUPPORTS

Figure 3.24   Column heads suspension system

$\frac{1}{4}$" STRAND

CHUCK

C6x8.2

C6x8.2

W4x7.7

L1"x4"x6"

6"

6"

8"

4"

28"

32"
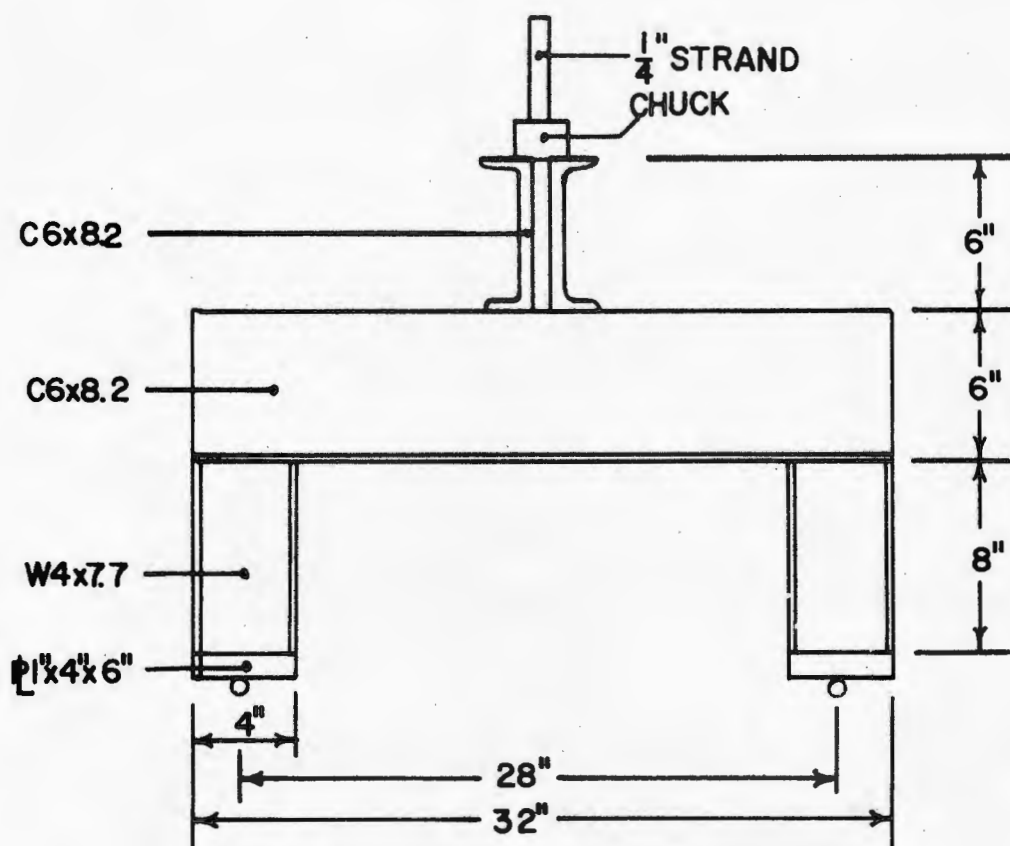
a)   SCHEMATIC DIAGRAM OF BEAM HEAD
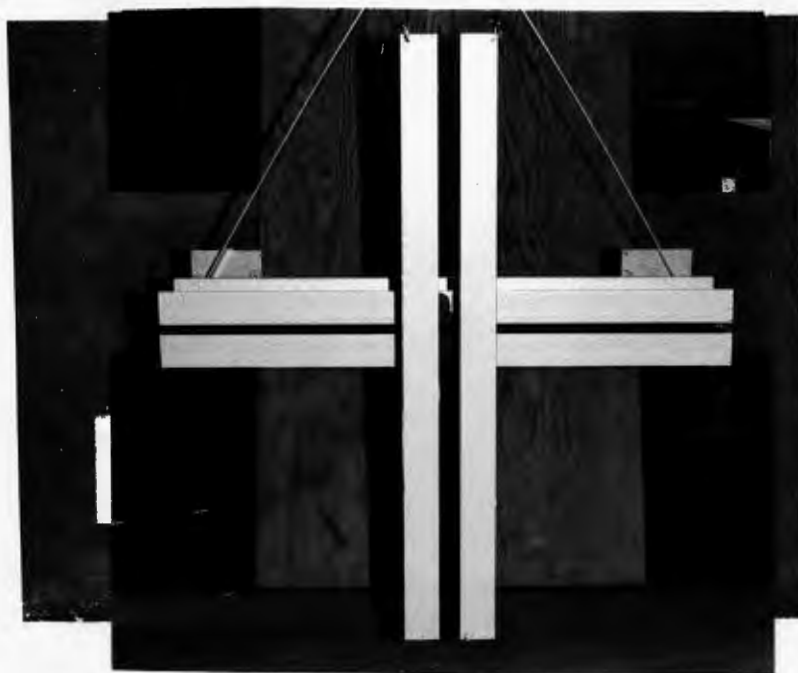
Figure 3.25   Beam head
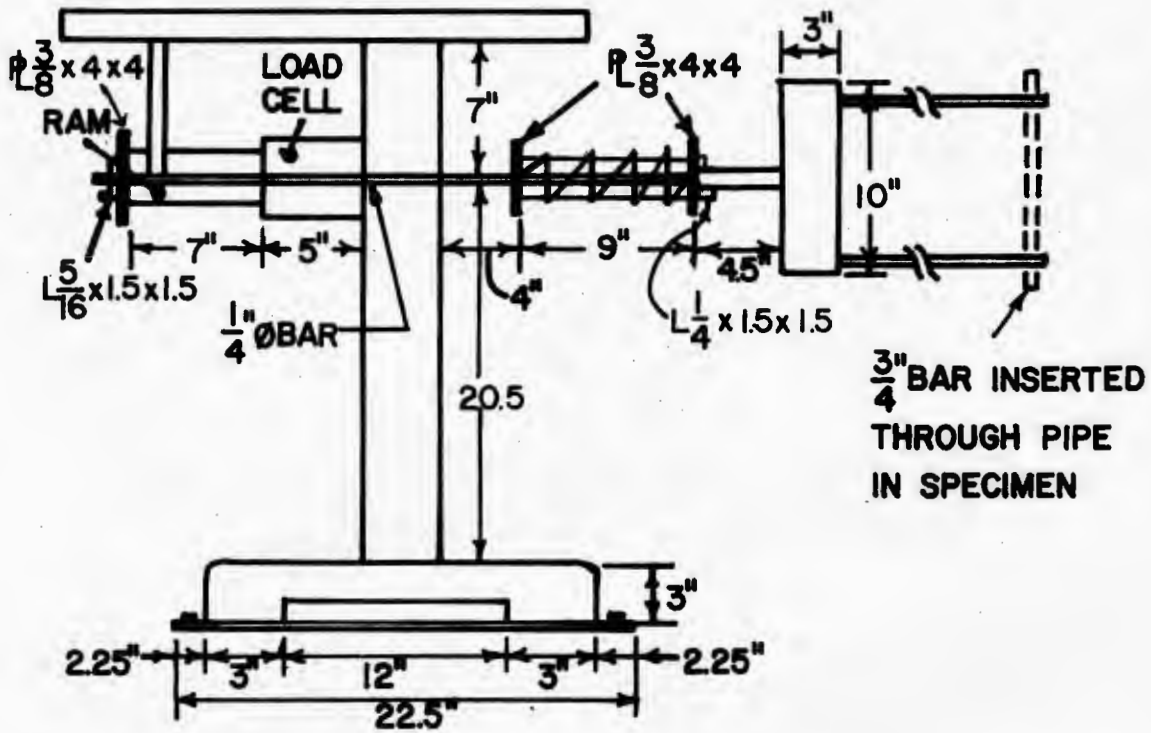
a) SCHEMATIC DIAGRAM
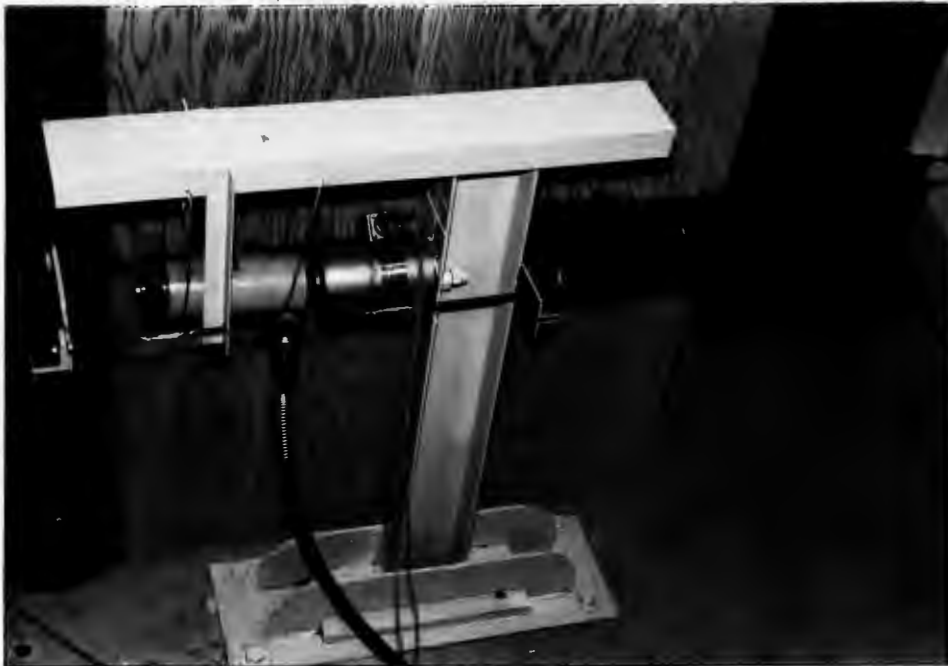
b) LATERAL LOAD SYSTEM

Figure 3.26 Lateral load assembly

welded to a steel plate PL 3/8" x 4" x 4". The lateral load ram assembly consisted of two steel angles connected together by two adjustable steel bars (1/4"∅), a 10-kip capacity load cell, and a 12-kip capacity ram. This assembly was supported by a stand that is bolted to the concrete slab. A snapshot of lateral load assembly is shown in Fig. 3.26(b).

CHAPTER IV

TEST RESULTS AND PREDICTED BEHAVIOR

4.1   GENERAL

As the experimental portion of this investigation, two rectangular reinforced concrete frames were designed based on two different methods, and tested to failure. One frame was designed by the ultimate strength design method prescribed by ACI 318-71 (10), the other by a limit design method. These two frames are designated as USD-2 and LD-2 respectively. The schematic diagram and principle properties of the frames are shown in Table 3.1.

For the reduction of all data, a computer program called "FRAG∅" was used. This program calculates the moment acting at a section for an applied axial load and measured concrete surface strain at that section. The input information for "FRAG∅" consists of section properties, the axial load on the section, the dial gage readings from curvature meters, and curvature meter arm lengths. The output includes the curvature, the axial load computed by integrating the concrete stress block over the cross section, the moment computed at the section corresponding to the input axial load and finally the moment computed by integration of stress block.

The experimental results for each frame are presented essentially in the form of six graphs as follows:

a) Load vs. Moment. These graphs show the axial column load and

sway load vs. the indicated moments. The first graph shows the axial column load vs. the moments at corners B and C for the columns; and the second graph shows the lateral load vs. column and beam moments at corners B and C. Column axial loads and the lateral load were measured using pressure transducers and a load cell, respectively. From the dial readings of each pair of curvature meters at a station, the bending moments were computed at mid point of that station using program "FRAGØ". There were four stations along the beam and two stations along each column.

If the column axial loads had no accidental eccentricities, then the beam and column moments would be exactly the same at beam and column centerlines. However some inequality was observed which was partly due to the fact that cracked beam stiffness is assumed by "FRAGØ"; and partly due to the accidental eccentricity of the column axial loads.

b) Lateral Force vs. Components of Moment. This graph shows the measured lateral force vs. components of moment on the leeward column which are the moments due to beam loads Q, lateral force H, and sway deflection.

c) Lateral Force vs. δ. This graph shows the measured lateral force vs. the moment magnification factor δ for the leeward column. The moment magnifications factor δ is obtained from the relationship $\delta = M_T/(M_T-M_{P-\Delta})$; where M_T is the total moment on the leeward column due to the beam loads Q, lateral force H, and sway deflection; and $M_{P-\Delta}$ is the moment due to sway deflection.

d) Load vs. Corner Rotations. This graph shows the measured column loads and sway load vs. corner rotations measured at corners A

and D using dial gage systems.

e) <u>Load vs. Lateral Deflection</u>. These figures show the lateral deflection measured at corner B vs. the axial loads and lateral load for each frame. Theoretically, no lateral deflection under gravity loads was expected. However, some deflection under gravity loads was observed which is due to imperfection in frame geometry or loading.

4.2   FRAME USD-2

a) <u>General</u>. Frame USD-2 was a symmetrical frame, designed by the Ultimate Strength Design method. It represented the lower level of a seven-story unbraced frame with the beam to column load ratio of $Q/P = .083$ as discussed in Chapter 2. The columns were 4.00 in. deep by 6.00 in. wide; and the beam was 4.5 in. deep by 6.00 in. wide. Column reinforcements were 4-#3 longitudinal bars and #12 gage wire ties at 4.00 in. intervals. Concrete strength for columns was 4610 psi on the day of testing. The beam was also reinforced with 4-#3 bars tailored according to the moment envelope and, tied with #12 gage wire stirrups at 1.90 in. intervals. Compressive strength of the concrete for the beam was 4498 psi.

Frame USD-2 was designed such that the frame failure would occur as a result of hinges developing in the beam. The loading was based on the actual design loads. Column loads P were applied at 2-kip increments, and Q/P ratio of .083 was maintained all during the test. After reaching the maximum gravity loads, beam and column loads were held constant and sway load was applied at 200 lb. increments until failure. After frame failure, lateral load was taken off, and the gravity loads were reduced by 25%. Lateral load was reapplied incremen-

tally and only the lateral deflection readings were recorded. Lateral

load was increased again until frame became completely unstable.

b) Load vs. Moment. Axial thrust vs. the indicated column corner

moments at corners B and C are shown in Fig. 4.1. The applied column

loads P were increased to 23.4 kips and each beam load Q to 1.93 kips,

to result in total column thrusts of 25.33 kips. As shown in Fig. 4.1,

at maximum column thrust of 25.33 kips, column corner moments are 30 kip-in.

The gravity loads were held constant during subsequent application of

lateral load H which increased the moment at column corner C to M_p =

58 kip-in.

Lateral force H vs. the indicated moments in the beam and

columns are shown in Fig. 4.2. Theoretically the beam and column end

moments would be exactly the same under gravity loads. However, as

indicated in Fig. 4.2 some inequalities between the beam and column

end moments were observed which are due to accidental eccentricities,

difference in shear forces acting at two faces of the joint block, and

cracked beam stiffness assumption by "FRAGØ".

As indicated in Fig. 4.2 the beam and column moments at corner

C were increased almost linearly up to 2400 lb. At this level excessive

cracking was observed at corner C. It appears that at 2500 lb. the beam

reached its maximum moment capacity at corner C and developed the first

hinge. At the next increment large cracks appeared at poing M' (steel

cut off point). The load increment was then decreased to 50 lb. It

appears that at 2850 lb. point M' is very close to its maximum capacity

while corner C of beam was still resisting the constant hinge moment.

Thus with two hinges in the beam, first hinge at corner C and the second

hinge at point M', the frame became unstable.

c) Lateral Load vs. Components of Moment. Lateral load vs.
components of moment on leeward column is shown in Fig. 4.3. The moment
induced on the leeward column comes from three sources; (1) moment from
beam loads Q, (2) moment from the lateral load H, and (3) moment from
the sway deflection. The value of M_Q using elastic analysis is M_Q =
.19QL = 0.19 x 1.93 x 84 = 30.8 k-in. at center of joint block; or
30.8 x 18.75/21 = 27.5 k-in at the face of the beam; and M_H = Hh/2.
The indicated M_Q progressively decreases as the lateral force increases.
This in part is due to the decreasing stiffness of the column as the
moment increases. The lower stiffness of the column thus causes a
smaller amount of beam load moment to be transferred to the column.

d) Lateral Load vs. δ. As shown in Fig. 4.4, the moment magnifi-
cation factor δ increases linearly up to H = 2400 lb; but because of
larger $M_{P-\Delta}$ at higher loads, the curve tends to become flatter at
loads higher than 2400 lb. At H = 2850 lb, the $M_{P-\Delta}$ was 9.9 in-k,
out of a total moment of 61.5 in-k; so the indicated magnification
factor δ was 61.5/(61.5-9.9) = 1.19.

e) Corner Rotations. The axial load and lateral force vs. the
measured rotations at corners A and D of the frame is shown in Fig. 4.5.
Corner rotation increased almost linearly up to 2400 lb, and the curves
became flatter at higher loads. Rotation of corner D was slightly
higher than the rotation of corner A.

f) Load vs. Lateral Deflection. The measured and computed load
deflection curves are shown in Fig. 4.6. As discussed earlier in
section 4.1-e, since frame USD-2 was symmetrical no lateral deflection

under gravity load was theoretically expected. However as indicated in
Fig. 4.6, a lateral deflection of .002 in. (to the right) occured at
maximum gravity loads. The measured initial stiffness of the frame was
higher than the analytical curve. This might be expected since tensile
strength of the concrete as it affects the beam stiffness was neglected
in the analytical computer program. Computer results indicated that
the frame failure would occur at H = 2400 lb. The actual frame withstood
a maximum lateral force of 2850 lb. After reaching the maximum lateral
force of 2850 the lateral load was released followed by decreasing the
gravity loads by 25%. Lateral load was applied again and the reloading
response is also shown in Fig. 4.6. As indicated, frame was capable of
resisting a lateral load of 1800 lb. before becoming unstable.

Figures 4.7 and 4.8 show four photographs of the frame after
failure.
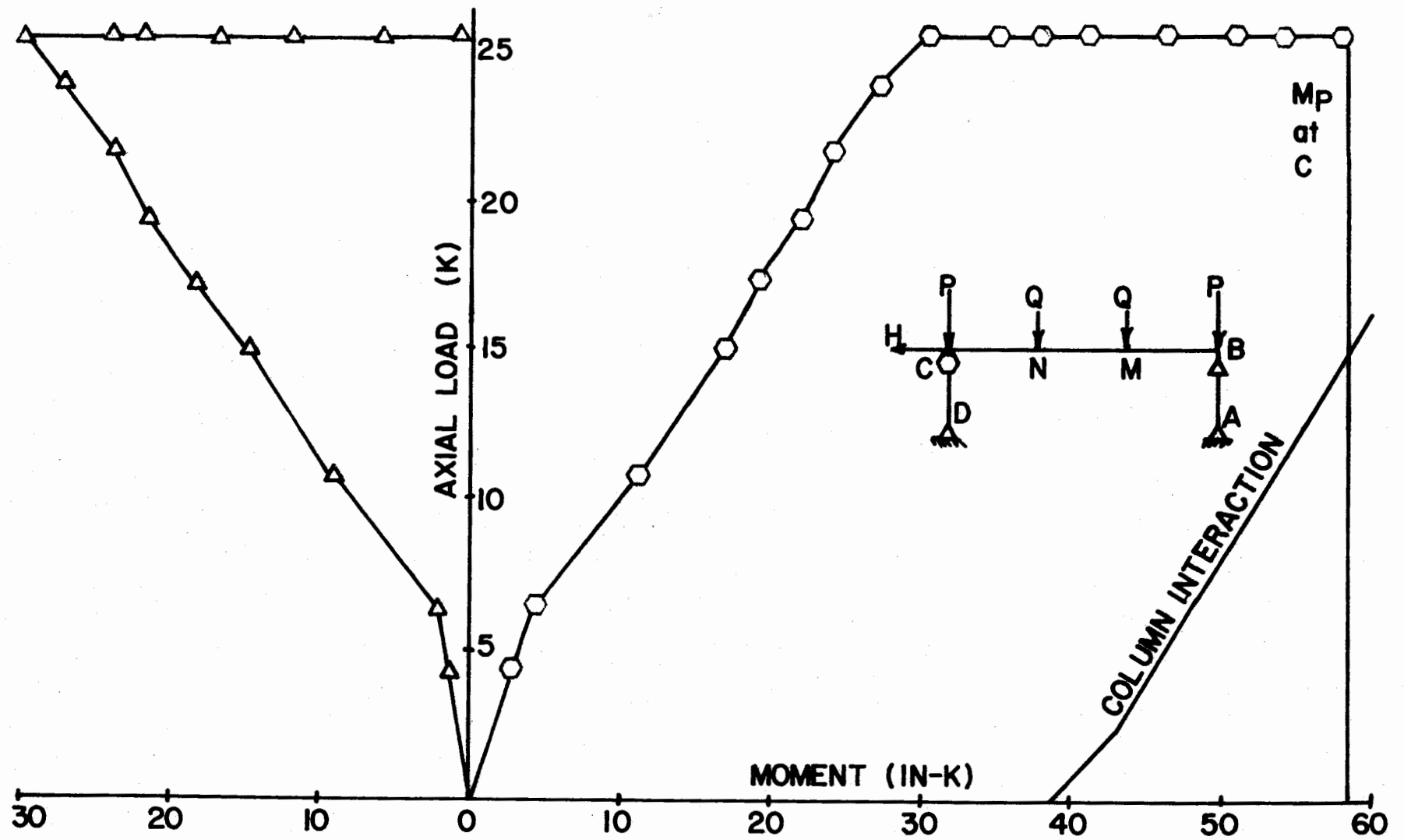
Figure 4.1 Axial load-moment relationship, frame USD-2
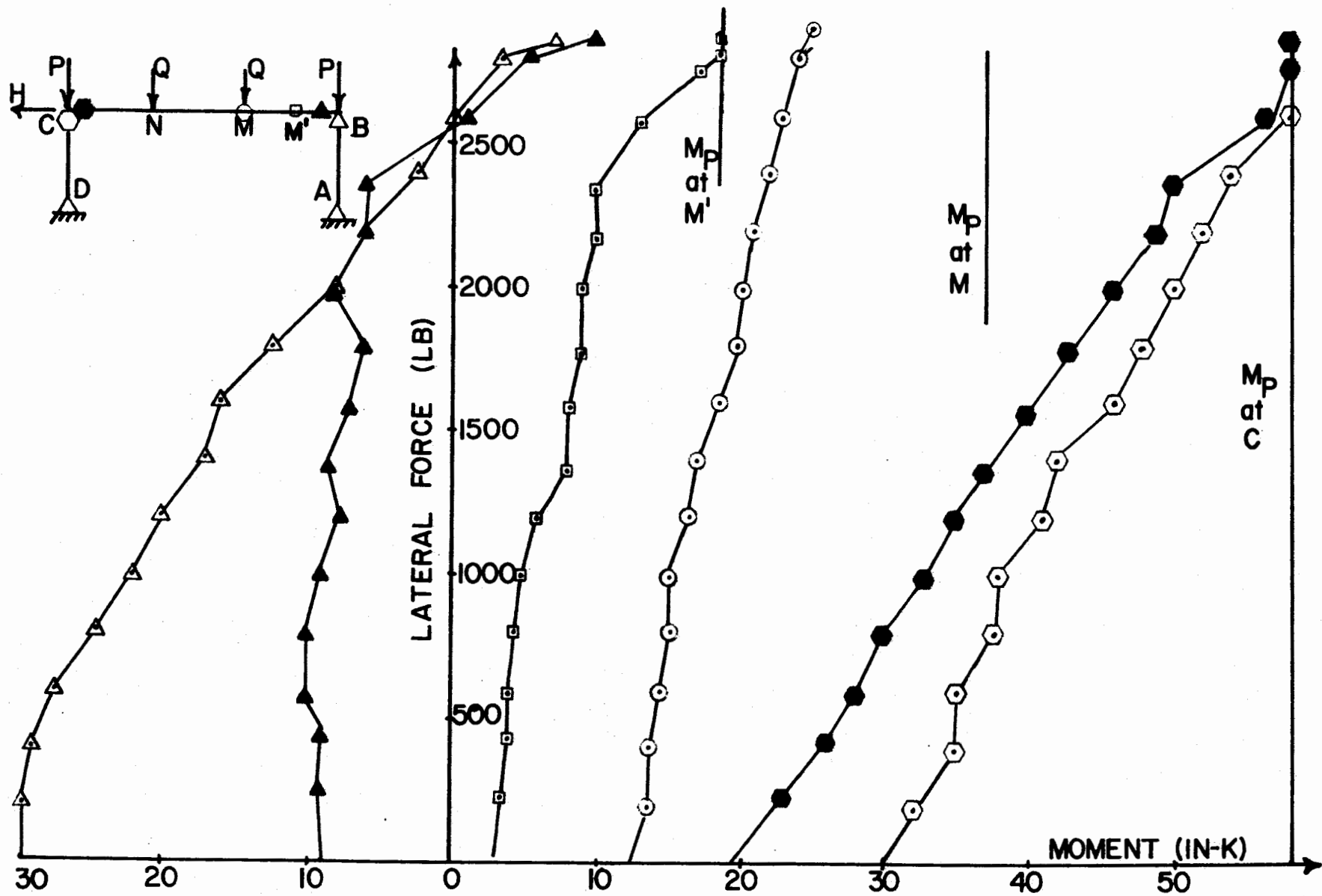
Figure 4.2 Lateral force-moment relationship frame USD-2

Figure 4.3 Components of moment in left column, frame USD-2
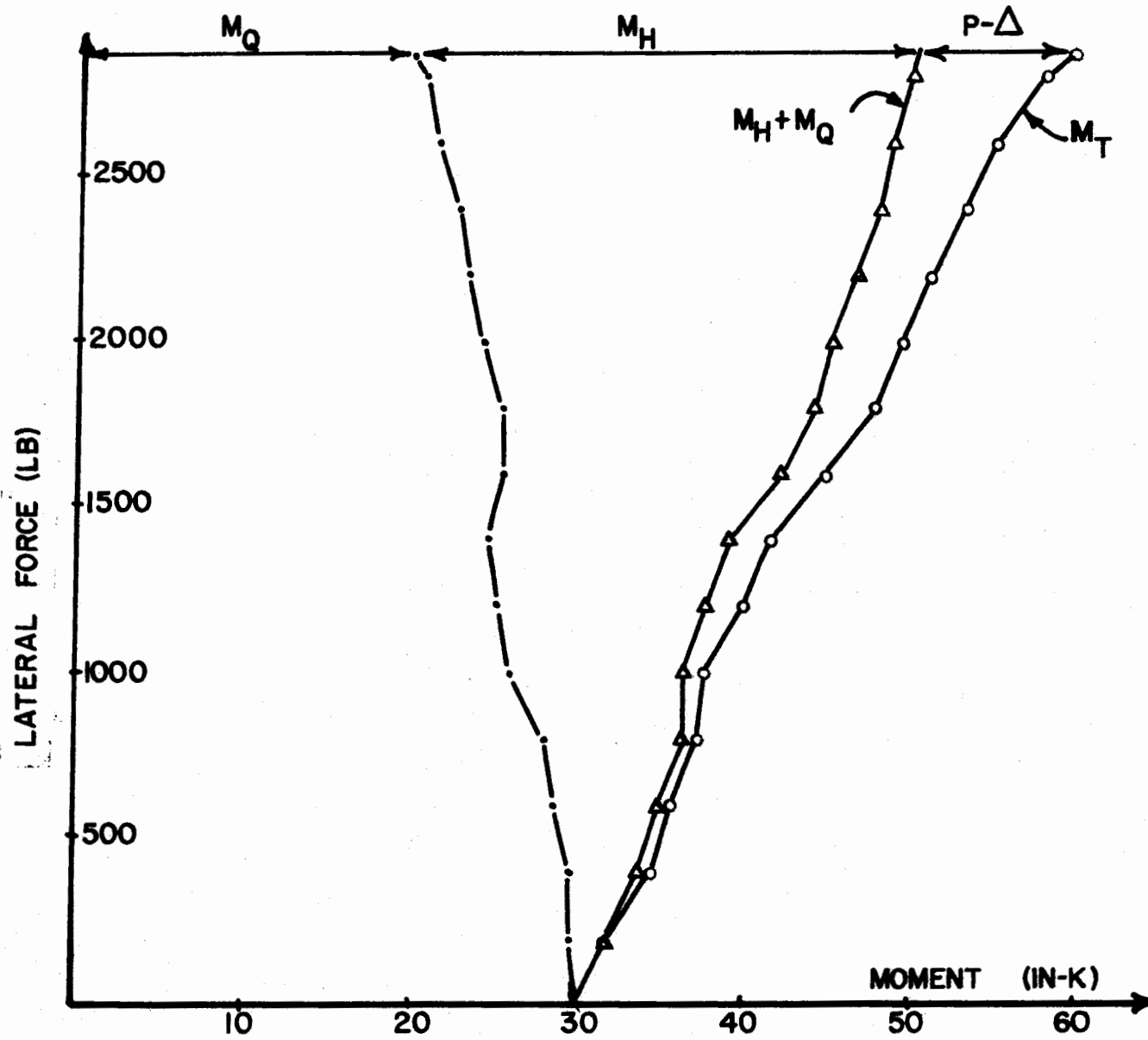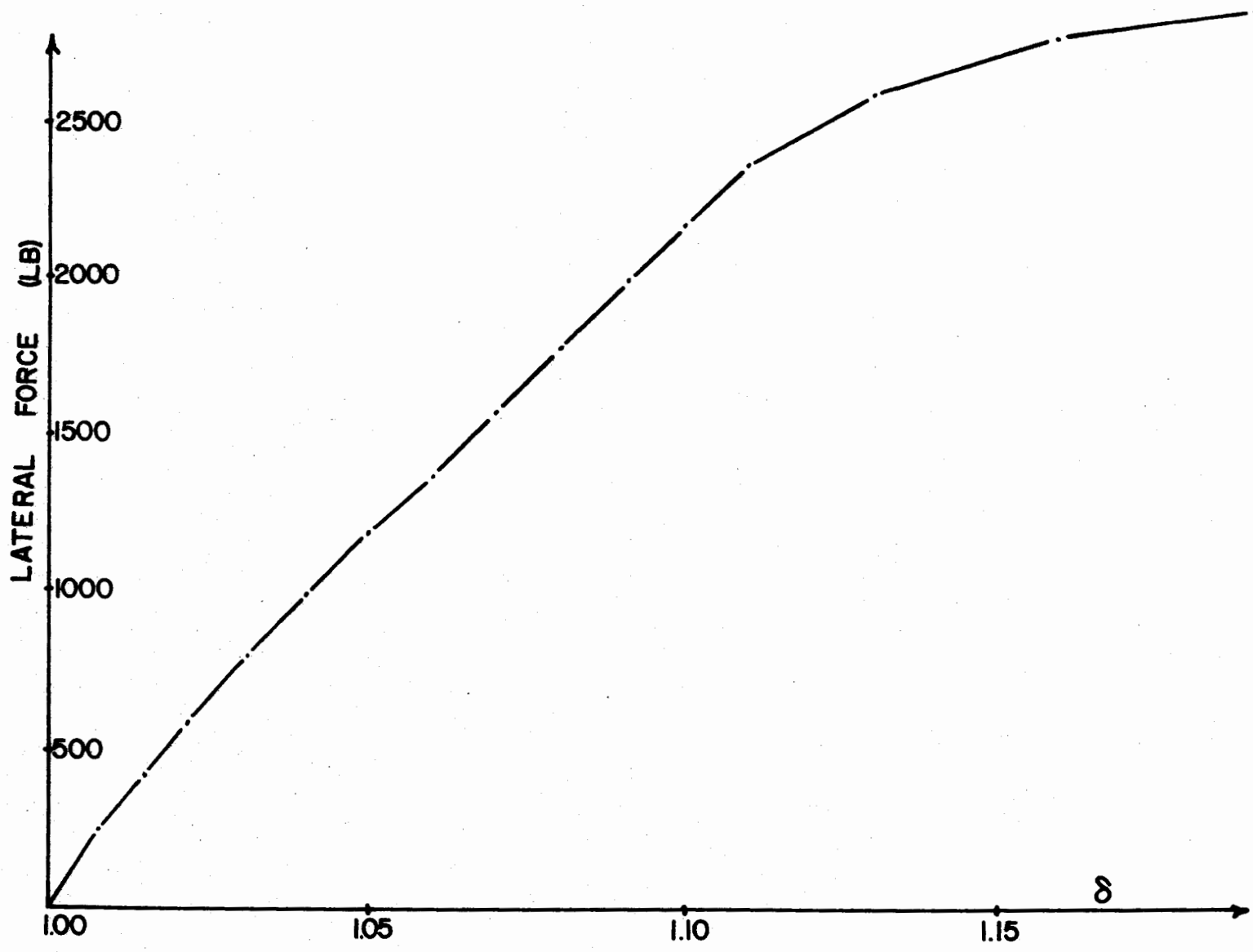
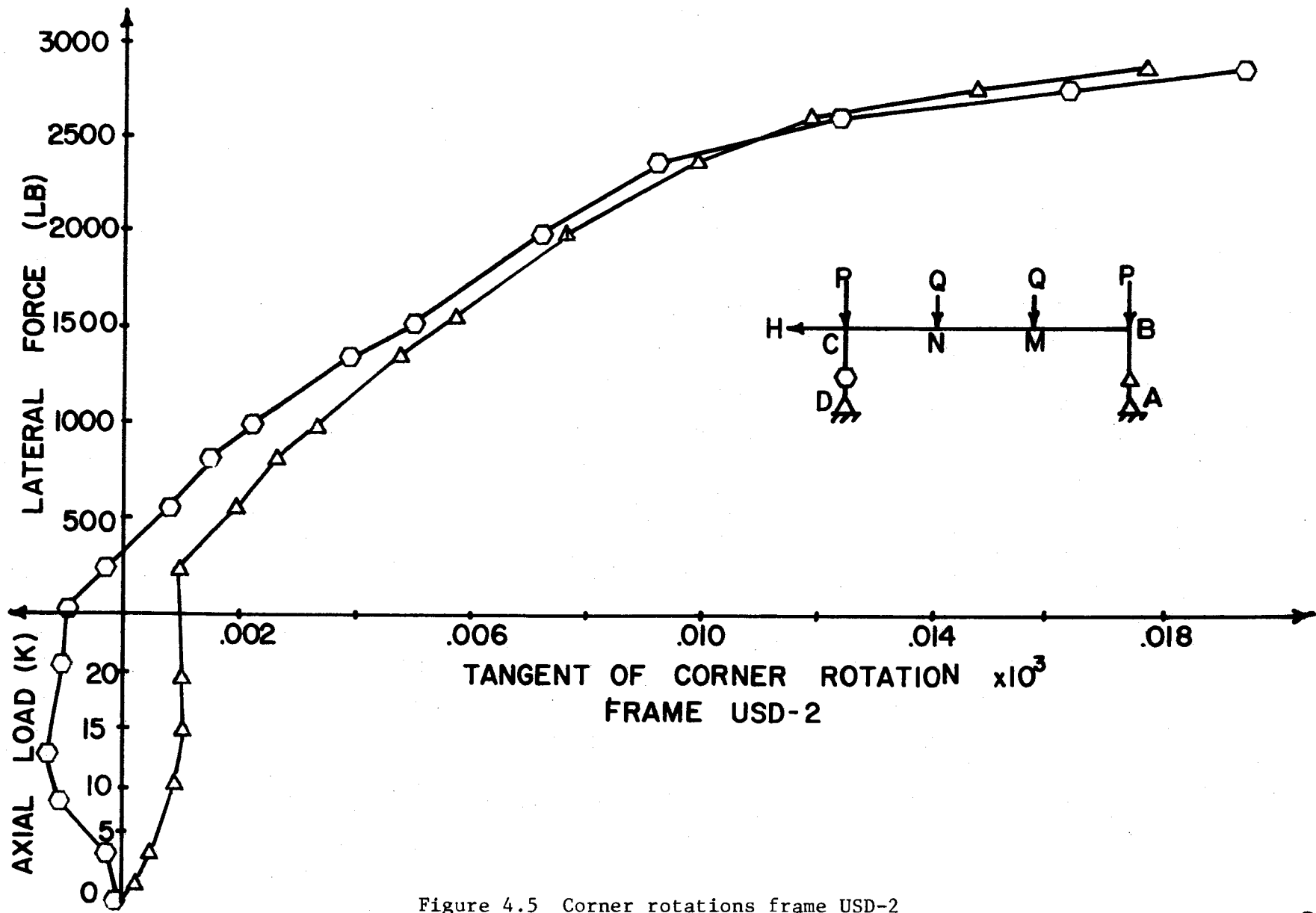Figure 4.4 Lateral force-δ relationship, frame USD-2

Figure 4.5   Corner rotations frame USD-2
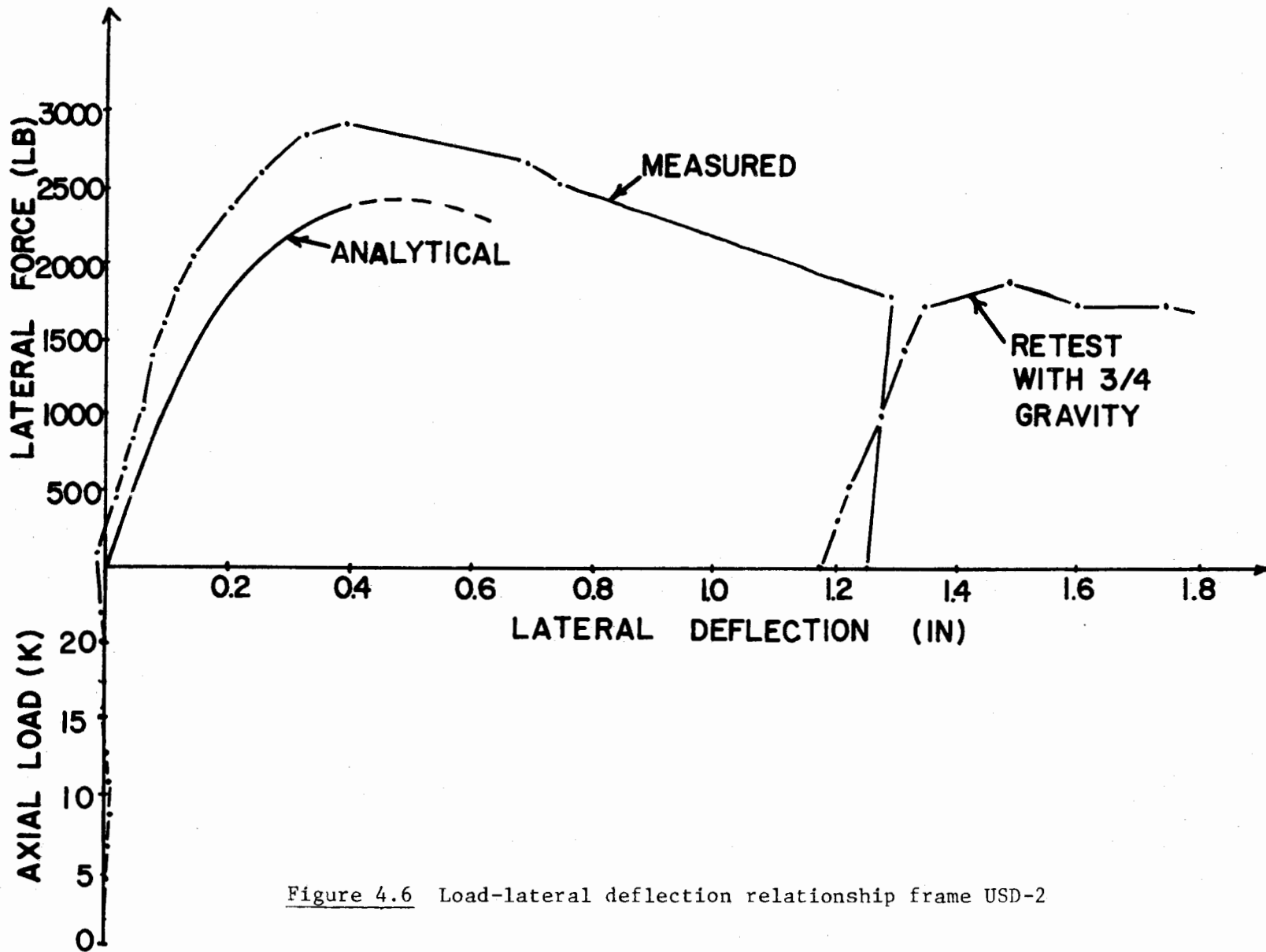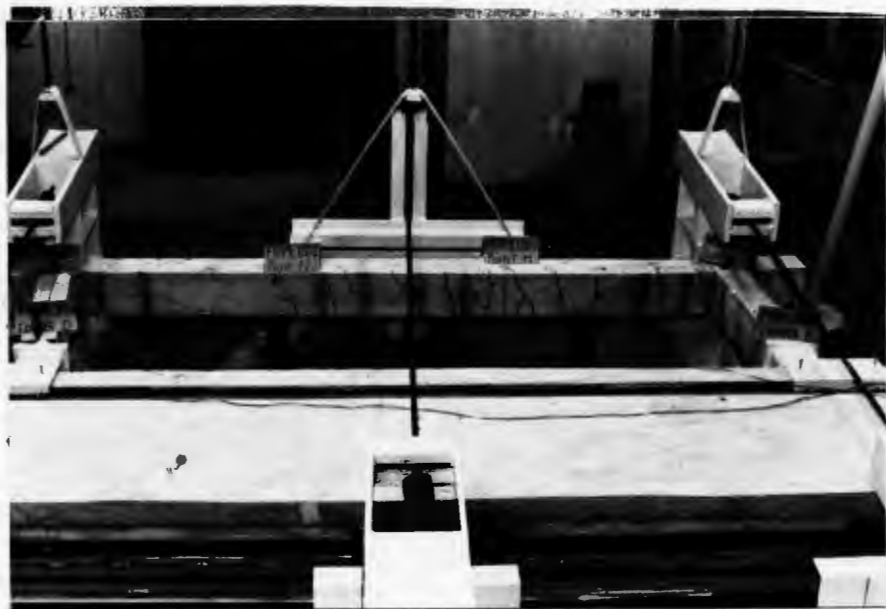
Figure 4.6 Load-lateral deflection relationship frame USD-2

(a)   OVERALL VIEW OF FRAME USD-2

(b)   CORNER C

Figure 4.7 Two views of frame USD-2 after testing

(a) CORNER B

(b) CRACKS AT THE BEAM

Figure 4.8 Two views of frame USD-2 after testing

4.3   FRAME LD-2

a) <u>General</u>. Frame LD-2 was a symmetrical frame, designed by a limit design method. It represented the lower level of a seven-story unbraced frame with the beam to column load ratio of $Q/P = .083$. The columns were 3.50 in. deep by 6.00 in. wide; and the beam was 4.50 in. deep by 6.00 in. wide. Columns reinforcements were 4-#3 longitudinal bars and #12 gage wire ties at 4.00 intervals. Concrete strength for column was 4372 psi on the day of testing. The beam was also reinforced with 4-#3 bars tailored according to the moment envelope and tied with #12 gage wire stirrups at 1.87 in. intervals according to the shear requirements.

Frame LD-2 was designed such that the frame failure would occur as result of hinges developing in the beam. Column loads P were applied at 2-kips increments and Q/P ratio of .083 was maintained all during the test. After reaching the maximum gravity loads, beam and column loads were held constant and sway load was applied at 200 lb. increments until failure.

b) <u>Load vs. Moment</u>. Axial thrust vs. the indicated corners moments at corner A and B are shown in Fig. 4.9. The applied column load P was increased to 23.57 kips and beam loads Q to 1.98 kips, to result in total column thrust of 25.57 kips. As shown in Fig. 4.9, column moments at corners B and C increase almost linearly with each load increment until the lateral load was applied. The gravity loads were held constant during subsequent application of lateral load H, which increased the moment at column corner C to $M_p = 46$ in-k.

Lateral force H vs. the indicated moments in the beam and columns are shown in Fig. 4.10. The initial lateral load increment was 200 lb. As shown in Fig. 4.10, the indicated moments at corner C for beam increased almost linearly until H = 1800 lb. At this load the beam reached its maximum moment capacity at corner C, and excessive cracking for this region was observed. At H = 2300 lb. extensive cracks developed in the beam at the negative moment steel cut off point (point N') near corner C. Fig. 4.10 shows that at this load the beam moment at corner B started to increase more rapidly. At H = 2400 lb. a tension crack appeared in the beam at corner B and the moment at this region appears to be close to its capacity. At H = 2430 lb. the frame became unstable, with vivid hinges at corner C and load point M.

c) Lateral Load vs. Components of Moment. Lateral load vs. components of moment on leeward column is shown in Fig. 4.11. The indicated moment in the leeward column are decomposed into three components: M_Q, M_H, and $M_{P-\Delta}$ following the procedure discussed in section 4.2(c). According to elastic analysis, M_H = Hh/2; M_Q = .19QL = .19 x 1.98 x 84 = 31.6 in-k at center of joint block, or 31.6 x 18.75/21 = 28.2 at the face of the beam. The indicated M_Q progressively decreases as the lateral force increases. This is due to the decreasing stiffness of the column as the moment increases.

d) Lateral Load vs. δ. The moment magnification factor δ vs. the lateral load is shown in Fig. 4.12. The curve is almost linear up to 2300 lb, and becomes very flat at higher loads. At H = 2430 lb, the $M_{P-\Delta}$ was 9.3 in-k, out of a total moment of 50 in-k; so the indicated magnification factor δ was 50/(50-9.3) = 1.23.

e) <u>Corner Rotations</u>. The axial load and lateral force vs. the measured rotations at corners A and D of the frame are shown in Fig. 4.13. The measured rotation of corner D was larger than the rotation of corner A, under maximum gravity loads. Rotations of corners A and D were almost linearly increasing up to 2200 lb of lateral load. The curve became much flatter at higher lateral loads, after the first hinge formation.

f) <u>Load vs. Lateral Deflection</u>. The measured and the computed load deflection curves are shown in Fig. 4.14. A lateral deflection of 0.03 in. was measured for this frame under maximum gravity loads. The measured initial stiffness of the frame appears to be higher than the analytical curve. The computer results (analytical curve) indicated that frame failure would occur at H = 1800 lb. The actual frame withstood a maximum lateral force of 2430 lb.

The frame was deflected under increasing lateral loads until a sway deflection of about 1 in. was obtained. Lateral load was then released followed by decreasing the gravity loads by 25%. Lateral load was applied again and the reloading response is also shown in Fig. 4.13. The damaged frame was capable of resisting 1800 lb before becoming unstable.

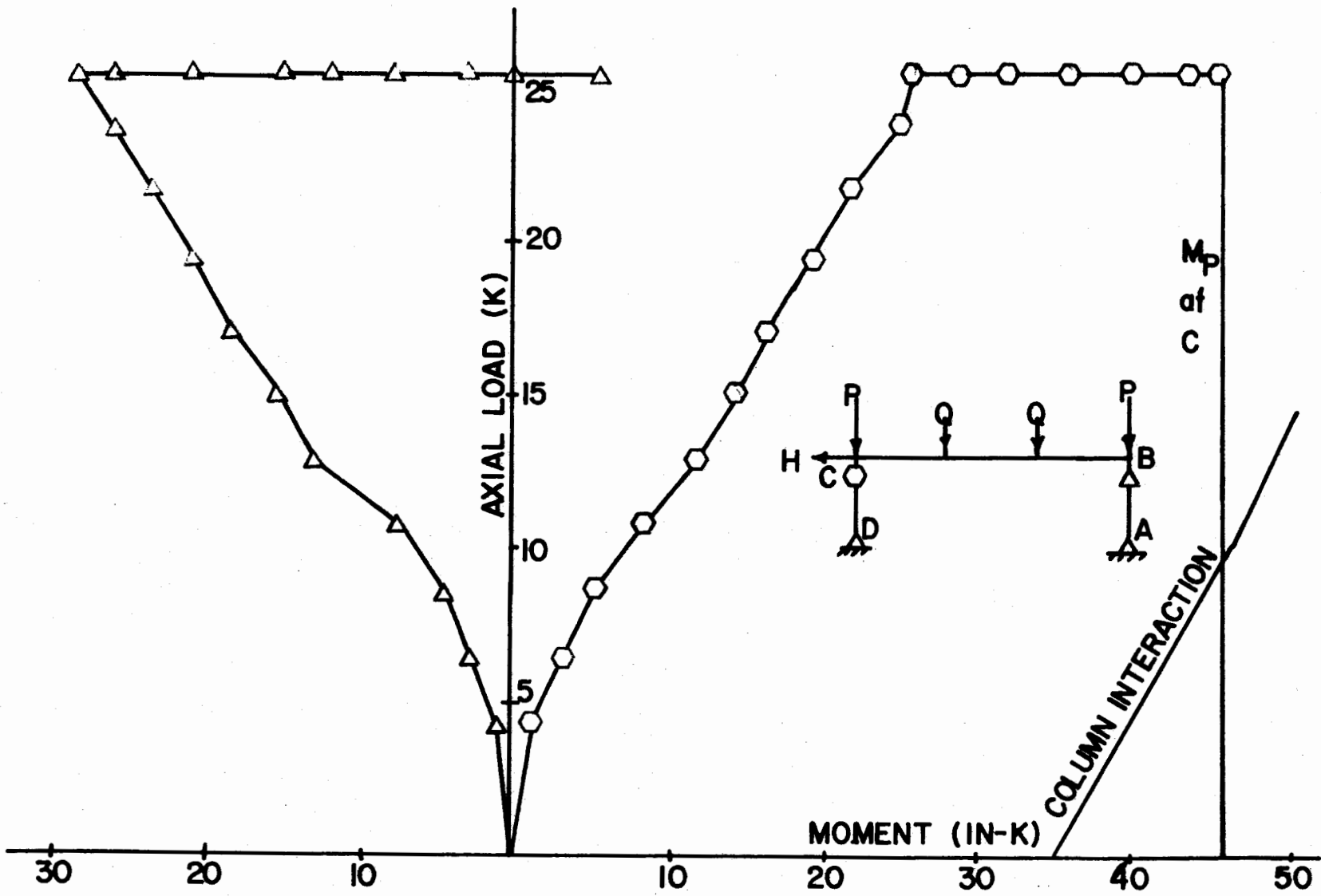Fig. 4.14 and 4.15 show four photographs of the frame after failure.

Figure 4.9   Axial load-moment relationship frame LD-2
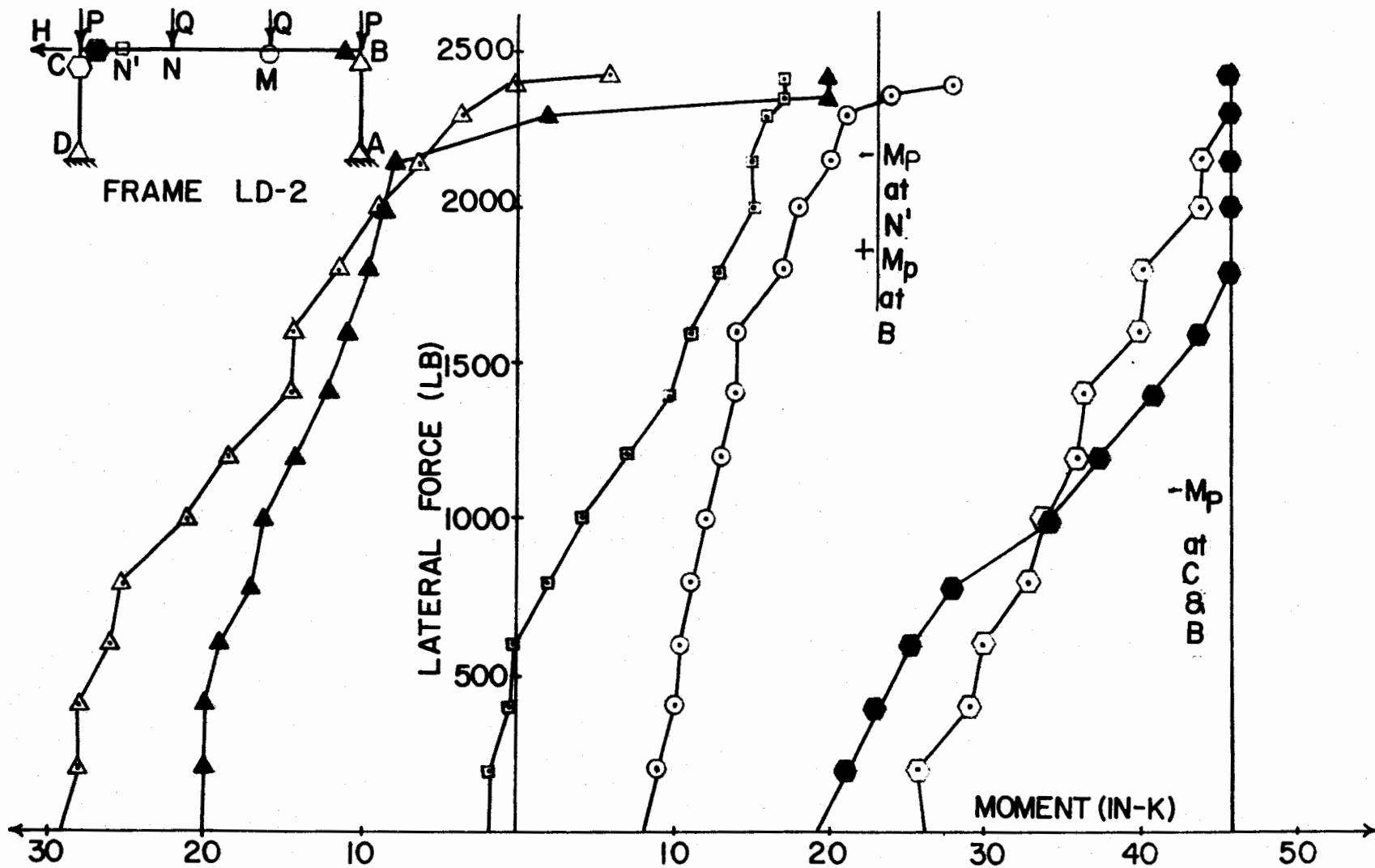
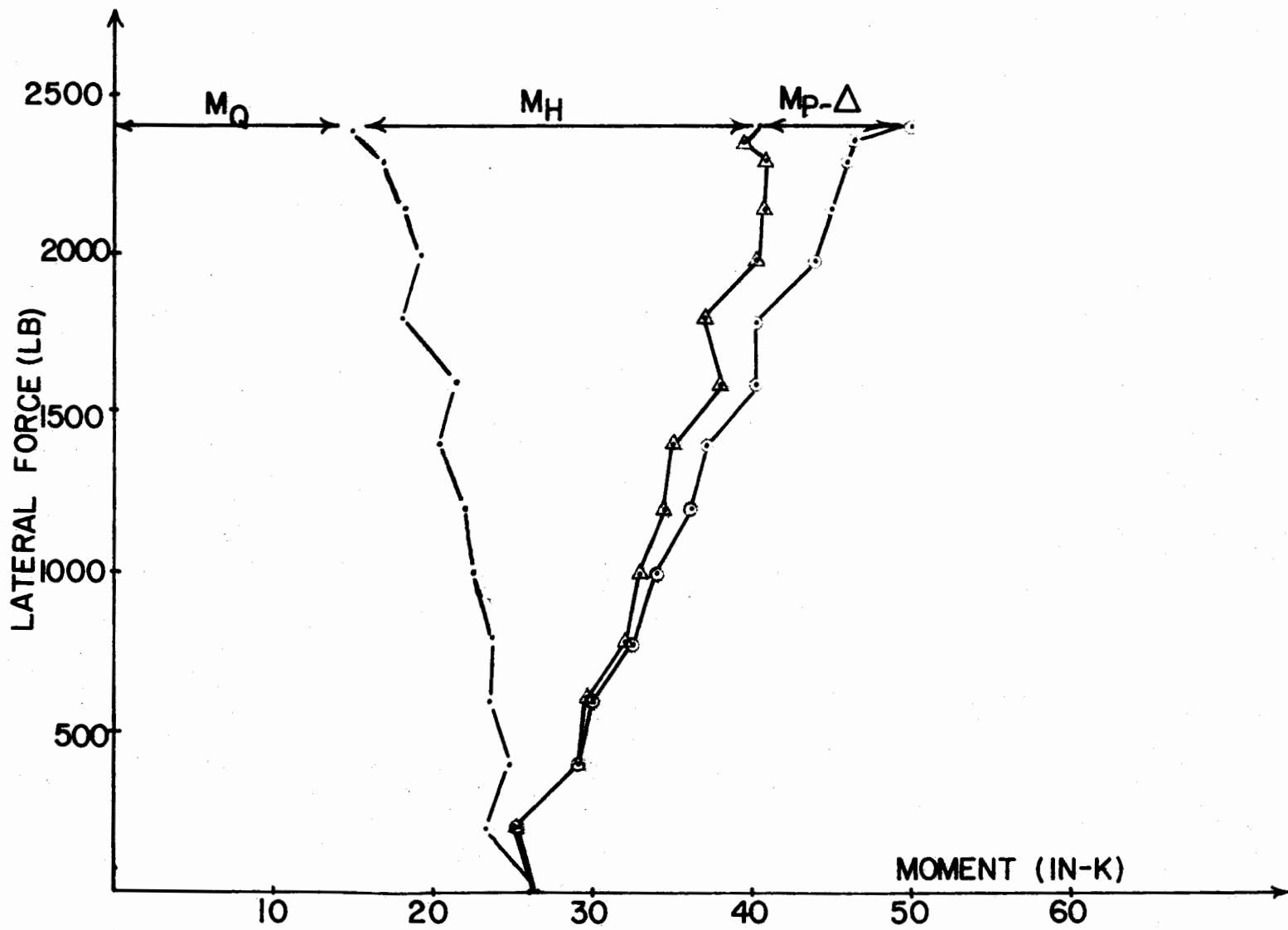Figure 4.10 Lateral force-moment relationship frame LD-2

Figure 4.11   Components of the moment in left column frame LD-2

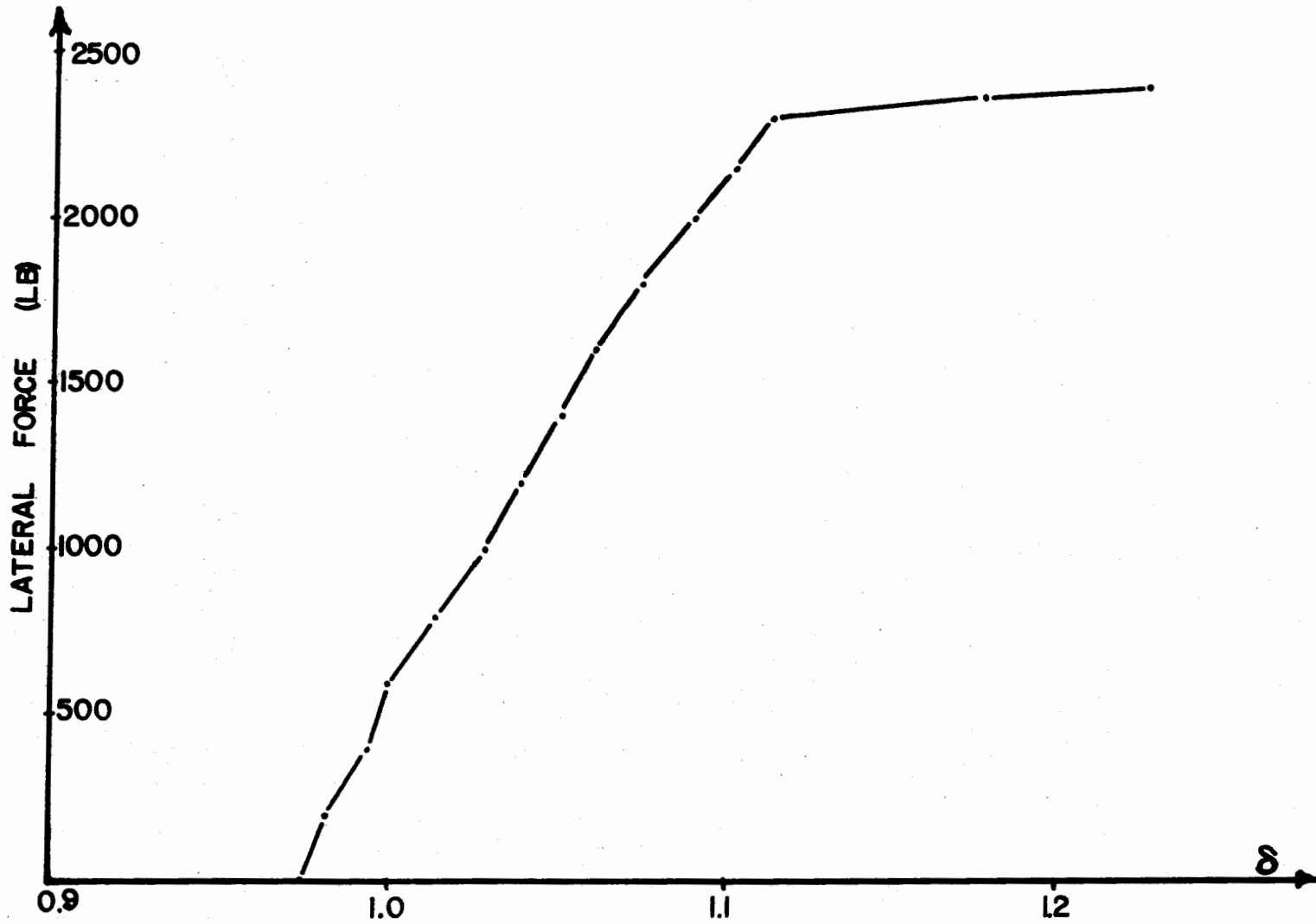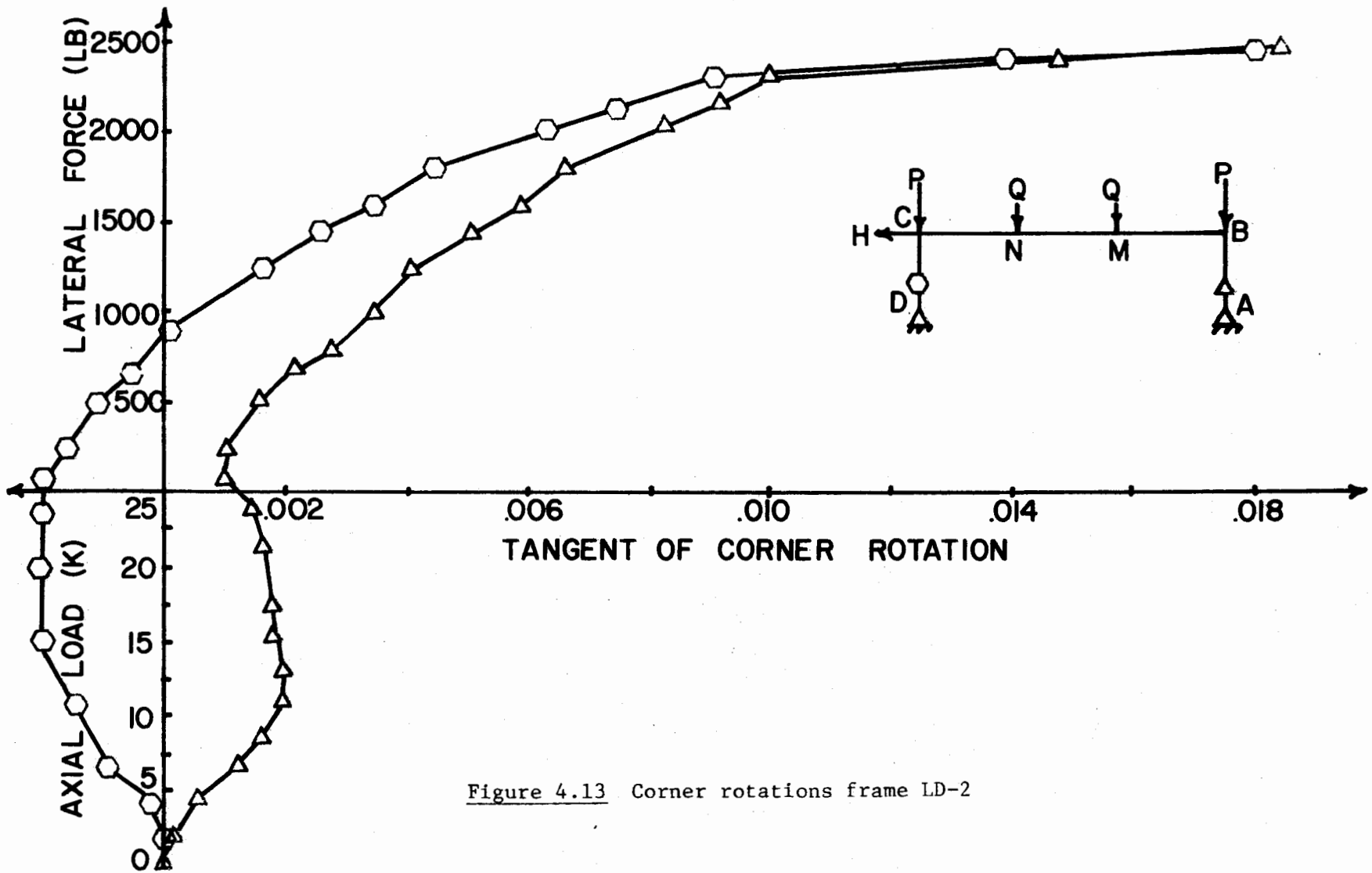Figure 4.12   Lateral force-δ relationship frame LD-2

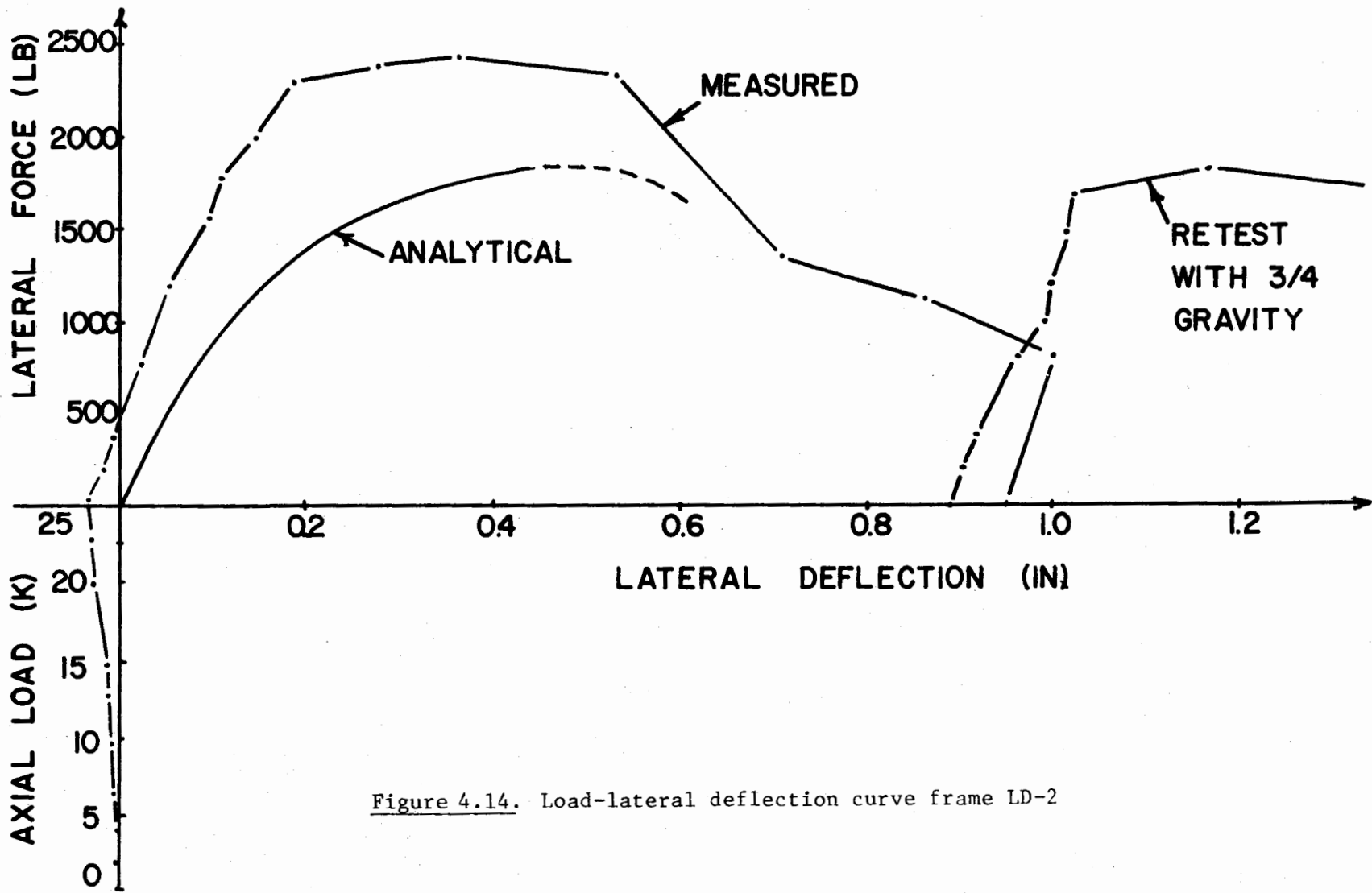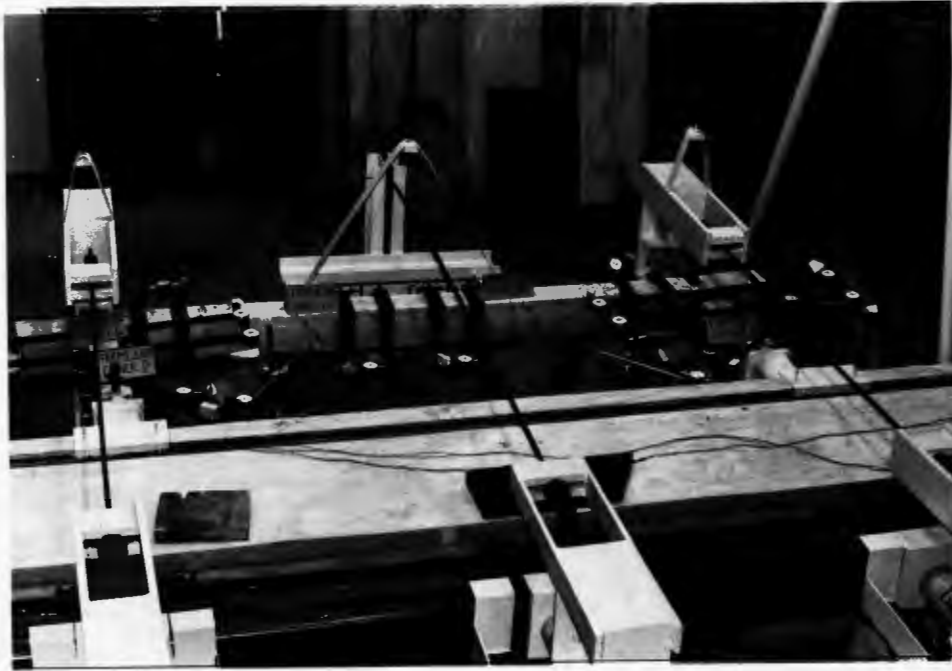Figure 4.13 Corner rotations frame LD-2

Figure 4.14. Load-lateral deflection curve frame LD-2

(a)   OVERALL VIEW OF FRAME LD-2

(b)   CORNER C

Figure 4.15   Two views of frame LD-2 after failure

4.4   <u>COMPARISON OF FRAMES USD-2 AND LD-2</u>

The lateral load vs. lateral deflection for frames USD-2 and LD-2 are shown in Fig. 4.17. As indicated in this figure, under service load H and factored load H, the measured lateral deflections for frame USD-2 and LD-2 were 0.11 in. and .175 in. respectively. At H = 2300 lb frame LD-2 stiffness started to decrease rapidly, and at H = 2430 lb this frame reached its maximum capacity and became unstable. Frame USD-2 reached its maximum capacity at H = 2850; i.e., its capacity was 17% higher than LD-2. The measured lateral deflection for frames USD-2 and LD-2, under maximum lateral loads were .390 in. and .366 in. respectively. As shown in Fig. 4.17, both frames continued to deflect under rapidly decreasing lateral loads.

The reloading responses for both frames under 3/4 of gravity loads are shown in Fig. 4.17. The damaged frames USD-2 and LD-2 were capable of resisting 1874 lb and 1800 lb of lateral load respectively before becoming unstable again. The reloading capacities were 66% and 74% of the original capacities respectively.
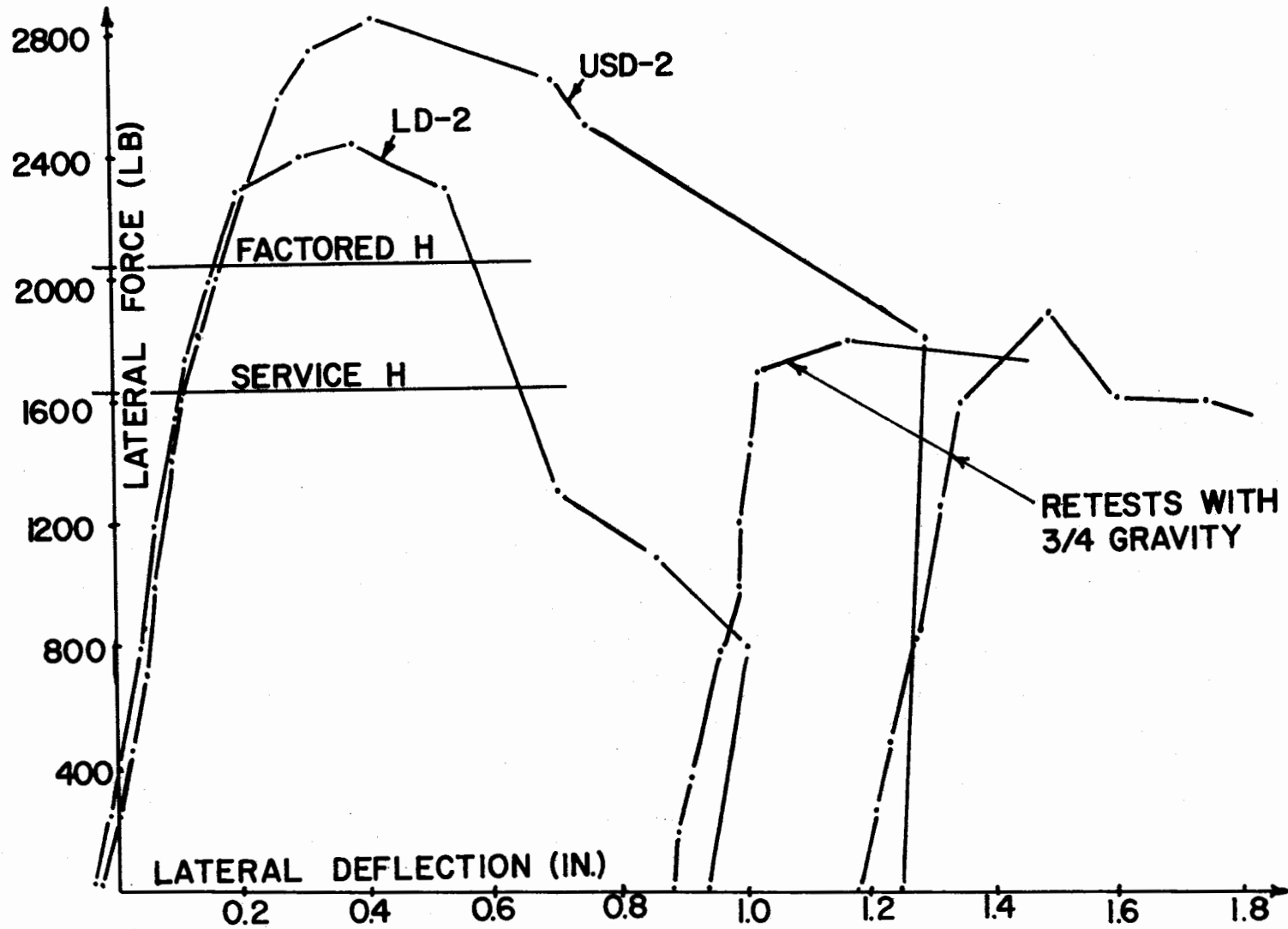
Figure 4.17   Lateral force vs. lateral deflection, frames USD-2 & LD-2

CHAPTER V

SUMMARY, CONCLUSIONS, AND RECOMMENDATIONS

The objective of this investigation was to determine the physical
behavior of single story, single bay reinforced concrete frames under
the action of low column axial loads, beam loads, and sway loads.
The investigation was carried out both analytically and experimentally.
The main analytical tool used in this investigation was the computer
program "NONFIX7", which is a generalized computational method for
nonlinear force deformation relationship and secondary forces due to
displacement of the joints during loading.

In the experimental portion of this investigation, two rectangular
frames, one designed by the Ultimate Strength Design method and the
other by a Limit Design method were prepared and tested to failure with
short time loading. Beam and column lengths were 84.00 and 21.00 inches
respectively. Frame loading consisted of column axial loads, beam
loads applied at third points of beam span, and lateral load. Column
and beam "gravity" loads were increased with constant beam to column
load ratio until the maximum design loads were reached. These loads
were then held constant while lateral load was applied until frame
failure. Based on the work conducted in this investigation, the
following conclusions are valid:

1) The loading system used in this investigation worked properly
    with no difficulty in operation and recording.

2) Under gravity loads, both test frames continued to resist increading lateral load even after the formation of one hinge at the leeward corner of the beam. The frames were still stable under increasing lateral load until a second hinge formed at an intermediate point in the beam. The frames with two hinges then became unstable.

3) The nonlinear computer program used to describe the general behavior of the frames in this investigation provided a reasonable estimate of ultimate capacity, deflection and mode of failure.

4) The moment magnification factors based on computations using the 1971 ACI building code and Merchant-Rankin formula reasonably predicted the measured values.

5) Frame stiffnesses were about the same for both frames, but frame USD-2 was capable of resisting 17% more lateral load than frame LD-2.

6) The maximum lateral load taken by each frame during reloading was on the average, about 70% of the original capacity.

In order to obtain information on validity of limit design concepts for more realistic unbraced frames, tests on rectangular multi bay-multi column concrete frames are recommended.

REFERENCES

1. Recommendation for an International Code of Practice for Reinforced Concrete, Committee European de Beton, Paris, 1964.

2. Baker, A. L. L., "Ultimate Load Design of Concrete Structures," Proc. Inst. Civil Engineers (London) 21 Feb 1962.

3. Mattock, A. H., "Rotational Capacity of Hinging Regions in Reinforced Concrete Beams," Flexural Mechanics of Reinforced Concrete, ACI SP-12, 1965, pp. 143-180.

4. Sawyer, H. A., "Comments on Model Code Clauses," ACI Journal, Sept. 1968, pp. 715-719.

5. Broms, B. and Viest, I. M., "Design of Long Reinforced Concrete Columns," ASCE Journal, Vol. 84, No. ST4, July, 1958.

6. Ferguson, P. M., and Breen, J. E., "Investigation of the Long Concrete Column in a Frame Subject to Lateral Loads," Symposium of Reinforced Concrete Columns, ACI SP-12, 1966, pp. 75-118.

7. Rad, F. N., "Behavior of Single Story Two-Column Reinforced Concrete Frames Under Combined Loading," Ph.D. dissertation, University of Texas, 1972.

8. Gunnin, B. L., "Nonlinear Analysis of Planar Frames," Ph.D. dissertation, University of Texas, January, 1970.

9. Honnested, E., "A Study of Combined Bending and Axial Load in Reinforced Concrete Members," University of Illinois Bulletin, Engineering Experiment Station Bulletin Series No. 399, November, 1951.

10. ACI Committee 318, Building Code Requirements for Reinforced Concrete (ACI 318-71), American Concrete Institute, Detroit, Michigan, 1971.

11. Gavin, T. G., "An Experimental Investigation of Unbraced Reinforced Concrete Frames," Thesis, Portland State University, May 1977.

12. Ferguson, P. M., Reinfroced Concrete Fundamentals, John Wiley & Sons, Inc., New York 1973.

13. ACI Committee 340, Ultimate Strength Design Handbook, SP. No. 17A, American Concrete Institute, Detroit, Michigan, 1968.

14. Wood, H. R., "Effective Lengths of Columns in Multi-story Buildings"
    Structural Engineering Journal, July 1974, No. 7, Volume 52,
    pp. 235-244.